MASTER

AERO-THERMODYNAMICS

SC-CR-68-3728 (P.t. 3)

September 1968

THREE-DIMENSIONAL INVISCID FLOW ABOUT SUPERSONIC BLUNT CONES AT ANGLE OF ATTACK

III: Coupled Subsonic And Supersonic Programs For Inviscid Three-Dimensional Flow

Prepared by
M. J. Abbett and R. Fort
General Applied Science Laboratories, Inc.

SANDIA LABORATORIES

DISCLAIMER

This report was prepared as an account of work sponsored by an agency of the United States Government. Neither the United States Government nor any agency Thereof, nor any of their employees, makes any warranty, express or implied, or assumes any legal liability or responsibility for the accuracy, completeness, or usefulness of any information, apparatus, product, or process disclosed, or represents that its use would not infringe privately owned rights. Reference herein to any specific commercial product, process, or service by trade name, trademark, manufacturer, or otherwise does not necessarily constitute or imply its endorsement, recommendation, or favoring by the United States Government or any agency thereof. The views and opinions of authors expressed herein do not necessarily state or reflect those of the United States Government or any agency thereof.

DISCLAIMER

Portions of this document may be illegible in electronic image products. Images are produced from the best available original document.

SC-CR-68-3728

THREE-DIMENSIONAL INVISCID FLOW

ABOUT SUPERSONIC BLUNT CONES AT ANGLE OF ATTACK

III. Coupled Subsonic And Supersonic Programs For
Inviscid Three-Dimensional Flow

September 1968

Prepared by

M. J. Abbett

and

R. Fort

General Applied Science Laboratories, Inc.

for

Sandia Laboratories

under

Contract Number 48-4014

ABSTRACT

The solution of the steady three-dimensional inviscid flow about supersonic blunt cones at an angle of attack is obtained by coupling a direct time-dependent solution for the subsonic portion of the shock layer with a steady state numerical afterbody solution.   An outline is given covering the coupling scheme and the use of the resulting Fortran computer code.

i

FOREWORD

This report compiles the work of G. Moretti, M. J. Abbett, G. Bleich, and R. Fort done under a Sandia contract (No. 48-4014). The aim of the contract was to develop a Fortran program which would determine the flow over a blunted cone in supersonic flow at an angle of attack. The contents of this report, developed in three sequential stages from February 1966 to July 1968, are presented here in a set of three volumes. Volume I, entitled "A Numerical Technique for the Three-Dimensional Blunt-Body Problem," develops the technique for handling three-dimensional flows. It includes a numerical model (cylindrical coordinates) for the nose region of a blunt body at an angle of attack. Upon using the resulting Fortran program it was found that the predicted pressure distributions were not accurate enough and the geometry of the downstream output surface was not easily adaptable to provide starting data for downstream supersonic solutions. In order to alleviate these problems, flow equations were re-derived using polar coordinates.

The reason for choosing the polar coordinate system is discussed in Volume II, "Improved Time-Dependent Techniques for the Blunt-Body Problem." A mathematical outline for this development is given. The resulting polar frame flow field does indeed improve the accuracy of the resulting flow properties and provides an output surface which can easily be used to start the downstream supersonic solution.

The development of the combined blunt body-afterbody solution is given in Volume III. This is entitled "Coupled Subsonic and Supersonic Programs for Inviscid Three-Dimensional Flow." In this volume the blunt-body solution is lined with a solution for the three-dimensional supersonic afterbody flow. It will calculate the flow over a blunted cone at an angle of attack. The solution can be extended downstream to approximately 20 to 30 nose radii and takes 40 to 60 minutes of CDC 3600 computer time depending on the body geometry and mesh spacing.

Roger R. Eaton - 9341

SUMMARY

The three-dimensional ideal gas flow in the shock layer of a blunted super-sonic cone at an angle of attack is calculated using two asymptotic solutions. The first solution calculates the steady state flow in the subsonic nose region by obtaining a time-dependent solution of the hyperbolic equations using numerical techniques. Internal, nonboundary points are calculated using a Lax-Wendroff numerical type technique. Boundary points, shock and body surface, are computed using a time-dependent method of characteristics. When a steady state solution is reached the flow properties on a surface of constant θ, (where the Mach number is everywhere > 1) are used for initial data for the afterbody solution.

The afterbody solution, using polar coordinates (r, θ, ϕ) assumes at r_o an arbitrary set of initial conditions provided by the nose region solution and computes the downstream flow as a function of $\theta, \phi,$ and r until an asymptotic state independent of r develops. The interior mesh points are again calculated using a Lax-Wendroff type technique and the boundary points by a method of characteristics.

This report covers the coupling of the time-dependent and radius (r) dependent solutions. Instructions are given for the operation of the resulting Fortran code. The type of input data required is detailed and sample output is provided. Output data is given in two sets of coordinates. One is wind orientated; the other set is given in body orientated coordinates. The analytical transformation from one coordinate system to the other is given.

TABLE OF CONTENTS

c_v	specific heat at constant volume
ℓ_o	reference length
L	distance from the origin of the wind-oriented blunt body coordinate system to the cone apex
M	Mach number
p	pressure
r_n	radius of the sphere
(r, θ, φ)	blunt body wind-oriented spherical polar coordinate system
(R, Θ, Φ)	body-oriented spherical polar coordinate system with origin at cone apex
R_i	value of R on cone initial data surface $(R_i = (1+\epsilon_6)R_{i_{min}})$
S	entropy
t	time
(u, v, w)	velocity components in the (r, θ, φ) coordinate system
(u_o, v_o, w_o)	velocity components in the (R, Θ, Φ) coordinate system
$(\bar{u}, \bar{v}, \bar{w})$	velocity components in the $(\bar{x}, \bar{y}, \bar{z})$ coordinate system
(u_2, v_2, w_2)	velocity components in the (x_2, y_2, z_2) coordinate system
XO	distance from ellipsoid (sphere) center or paraboloid focal point to the center of the (r, θ, φ) coordinate system

$(\bar{x},\bar{y},\bar{z})$ wind-oriented Cartesian coordinate system whose origin coincides with that of the (r,θ,φ) system

(x_2,y_2,z_2) body-oriented Cartesian frame centered at the cone apex

α angle of attack

β cone half-angle

ϵ_5 parameter used for determining $\left(\dfrac{\partial\Theta}{\partial R}\right)_{SHOCK}$

ϵ_6 parameter used for determining the initial cone data surface $(R_i = (1+\epsilon_6)R_{i_{min}})$

γ ratio of specific heats

μ viscosity coefficient

ρ density

I. INTRODUCTION

In this report we are concerned with the numerical computation of the inviscid flow past a blunt nosed cone. The problem is restricted in the following ways:

body: axisymmetric

blunted nose followed by a right circular cone*

cone tip is an ellipsoid (sphere) or paraboloid of revolution

continuous slope

gas: thermally and calorically perfect

constant specific heat ratio

inviscid (Euler equations)

uniform

aerodynamic: body flight speed is supersonic and steady

angle of attack not too large

Figure 1 illustrates the essential characteristics of the problem. The bluntness effect results in the bow shock being detached from the nose (on the scale being considered). A region of subsonic flow exists in the vicinity of the nose where the

---

* The solution is not continued downstream of the base of the cone.

Euler equations are <u>elliptic</u> in nature and the properly set

problem is of the boundary value type (for a steady flow). Some-

what downstream (as long as the angle of attack is not too large

and the Mach number is not too low) the flow becomes entirely

supersonic, the Euler equations are <u>hyperbolic</u>, and the initial

value-boundary value type of formulation is appropriate. Because

of the different mathematical and physical nature of the two

regions (but primarily because of the mathematical difference),

the usual procedure has been to split the problem into two pieces

which overlap where the flow is transonic ($M \sim 1$ but also $M > 1$).

If the flow is two-dimensional or axisymmetrical, there

are good ways to compute both the subsonic and supersonic regions.

The subsonic region can be handled in a number of ways, the most

successful being the unsteady direct method.* This method, in

which the steady solution is considered to be the asymptotic time

limit of an unsteady flow with steady boundary conditions, has

proven to be particularly successful since one can be certain

that as the mesh size decreases, the numerical solution of the

difference equations, providing they satisfy certain properties,

---

* In the direct problem, the body shape is specified and the shock
shape is found. In the indirect problem, one finds the body which
corresponds to a given shock shape; then the required shock for a
given body is determined by an iteration procedure.

converges to the solution of the Euler equations.* Usually the

method of characteristics is used to compute the supersonic

region since it is the most accurate numerical finite difference

technique for two-dimensional or axisymmetric supersonic flows.

The patching of the two regions does not present any particularly

excruciating problem.

In the case of three-dimensional supersonic blunt body

flows, the situation is considerably worse, the best solution

again being based on the unsteady method.[2]** In the supersonic

region, the method of characteristics can be used, though none

of the currently developed differencing schemes is completely

acceptable. However, in 1965 Moretti[3] developed a technique

---

* Though this has not been proven, there is every reason to
believe that "certain" is a justifiable word.

** 2) Superscripts refer to references listed at the end of
the report.

for computing the three-dimensional supersonic inviscid flow over a right circular cone at an angle of attack.* This technique can be used very well to analyze the supersonic flow region of a blunted right circular cone at an angle of attack.

This is a report on the coupling of the three-dimensional blunt body solution of Moretti and Bleich** with Moretti's cone at an angle of attack solution. With the resulting code one can compute the complete inviscid flow over a blunted cone at an angle of attack.

Before going into the details of the coupling, it is desirable to have a brief review of the analyses of the solution to be used for the blunt body and the cone at angle of attack problems. This is done in Section II, DIRECTION. In Section III are the analyses of the coupling and pertinent comments

---

* Actually, the technique is not restricted to right circular cones but is applicable to general three-dimensional smooth bodies having a preferred direction in which the flow component is supersonic. In fact, it has recently been applied at GASL to obtain the solution of the inviscid flow about non-circular quasi-conical bodies at angle of attack.

** Actually a modification of the computer program; see Ref. 4.

about the assumptions and restrictions of the analysis and computer codes. Results are given in Section IV along with a discussion of their significance, particularly with respect to the accuracy of the solution. For those who would like to use the code, an appendix is included in which instructions and advice are given.

II. DIRECTION*

Since the blunt body solution comes "before" the afterbody solution, let's discuss it first. We are concerned now with getting a good picture of the analysis used by Moretti and Bleich to obtain the solution of the steady, inviscid flow in the nose region of an axisymmetric blunt body at an angle of attack.

As previously mentioned, in regions of subsonic flow, the steady Euler equations are elliptic and lead to boundary value type problems. The boundary, in this case, is composed of the body surface, the sonic surface (i.e., the surface on which the fluid velocity equals the local sound velocity), and the detached bow shock wave. Unfortunately, neither the shock wave shape nor the sonic surface shape are known, a priori, so one is faced with solving a three-dimensional nonlinear elliptic boundary value problem with free boundaries. The manner in which this problem was conquered was by a diversionary tactic; the steady flow was considered to be the asymptotic time limit of an unsteady

---

* In this report when referring to the solution of the blunt body problem and the conical afterbody problem, we will always refer the blunt body solution to a spherical polar coordinate system (r, θ, φ) with lower case letters and the conical afterbody solution to a spherical polar coordinate system (R, Θ, Φ) with upper case letters.

flow. The reason for introducing the additional coordinate (four independent variables instead of three) is that the un-steady Euler equations are hyperbolic and lead to initial value-boundary value formulations. The mathematical and numerical treatment of such initial value problems is in a better state of development than it is for elliptic boundary value problems, and there are several ways of formulating a finite difference representation of the initial value problem which are amenable to numerical computation.

The main point of the analysis under discussion is that the flow field is divided into three regions; the shock wave, the body stream surface, and the interior flow, including all of the subsonic and a part of the supersonic flow. Thus, the domain of interest is extended beyond the steady state 'sonic surface'. For a discussion of this point see References 1, 2 and 4 (Figure 2).

Assuming the flow in the nose region to be completely known at a time t_o, the flow at a later time, $t_1 = t_o + \Delta t$, is obtained as follows. In the interior region the dependent

variables are expanded in a Taylor series in time centered at t_o.
Terms through the second order are kept, leading to a condition-
ally stable numerical scheme. The first order time derivatives
are computed directly from the Euler equations. The second
order terms are obtained by differentiating the Euler equations
with respect to time. When this is done, mixed derivatives in-
volving time and one of the space coordinates also appear. These
mixed time-space derivatives are evaluated by differentiating
the Euler equations with respect to that particular space vari-
able. At the shock and body points a clever characteristic
method is used. For further details of the method of solution,
see References 1 and 2. However, a couple of comments are now
in order.

Note that the Taylor series expansion is not done on
the divergence form of the Euler equations.[5-7] This should not
be a cause of worry since the virtue of the divergence form is
in computing flows with discontinuities. In that case, the
divergence form has the virtue of concentrating the region of
rapid change over a few mesh widths while maintaining a high
level of accuracy (relative to other mesh difference schemes).
Since the current analysis treats the shock as a discontinuity,

it is not necessary to be particularly insistent about using the divergence form of the equations.

The second point to emphasize is that on the entire outer boundary surface between the shock and the body, the flow must be supersonic. This is necessary in order to obtain the blunt body solution[1,2,4] (in addition, as will be shown below, it is necessary in order to couple the blunt body solution with that of the cone at an angle of attack).

So now we arrive at the discussion of the analysis for the supersonic flow about a pointed cone at an angle of attack and its relationship to the current problem. The steady inviscid supersonic flow about a pointed cone is conical. This enables one to eliminate one coordinate in a spherical polar coordinate system (R, Θ, Φ) centered at the cone apex, the "ignorable" coordinate being the radial one. The Euler equations then are considerably simplified and, if the angle of attack is not too large, are elliptic throughout in the two remaining independent variables. Again, we are faced with an elliptic boundary value problem with a free boundary, the shock. To make matters worse, there are two singularities (on the body in the windward and leeward symmetry planes) and a vortical

layer near the cone surface. The windward singularity causes no trouble, but the leeward singularity and the vortical layer are sources of big analytic difficulties. The result is that this problem, even at small angles of attack, has not been solved, though many people have made important contributions to the problem.

In 1965 Moretti first published* the results of an analysis which, though it does not solve the problem of the singularities, enables one to obtain a solution in the entire flow field, except in a neighborhood of the leeward singularity.** Because of the particular nature of the leeward singularity, Moretti was able to ignore it while still being able to get as accurate a solution as desired, within any given distance of the singularity, by just refining the mesh.** The idea is a child of that used to solve the blunt body problem: for general nonlinear problems, initial value formulations are often more

---

* As often happens, there is the Soviet counterpart to this work.[8]

** Of course, there are practical limitations on the refinement of the mesh; e.g. computer memory and speed limitations. The gross result is that the person with ordinary monetary and computing resources cannot get the correct entropy distribution near the body.

desirable (read solvable) than those of the boundary value type. Since the flow is supersonic, the Euler equations are hyperbolic with respect to the radial coordinate. So, why not get the conical solution as the limit, in R, of a nonconical flow? That is, we eliminated R to simplify the equations, so now put it back in so we can solve them! And that is what Moretti did. He divided the shock layer into three parts; the shock, the body stream surface, and the region between. The asymptotic solution is obtained by marching from one constant R surface to another. At each constant R surface, the region between the shock and the body is covered by a curvilinear mesh in the (Θ, Φ) coordinates. The solution for the interior region is obtained by expanding the dependent variables in a Taylor series in R. At the shock and body points a method of characteristics is used.

The obvious questions are: where does one start? how are the initial conditions obtained? The first part is straightforward; the flow is inviscid, so the length scale is essentially arbitrary and, so long as only the conical solution is of interest, it is only necessary to go far enough downstream (from some initial data surface) to get the desired

PAGES __12__ to __13__

WERE INTENTIONALLY

LEFT BLANK

III. ANALYSIS

A. General Comments, with Particular Attention to
    Layers and Singularities

It has been mentioned that we are concerned only with

inviscid flows. However, it should be noted that for given

Reynolds and Mach numbers, a flow may be satisfactorily treated

as inviscid for zero angle of attack and for small angle of

attack, but not for larger angles of attack. Of course, the

question is, what makes the angle of attack large? And the

answer is a function of many variables, but primarily the cone

semi-angle and the free stream Mach and Reynolds numbers (based

on the typical nose radius) in the current case. With this

oblique warning, viscous effects will not be subsequently men-

tioned.

There are two points to be considered with respect

to the inviscid solution, and they involve the entropy behavior

near the body and the bluntness-length ratio. The entropy layer

and leeward singularity are what make the pointed cone at an

angle of attack such a difficult problem. Moretti solved, in

principle,* the layer and bypassed the singularity in obtaining

---

* Because of computer limitations, his solution must be con-
  sidered to also bypass the layer, though, in principle, he
  can obtain the solution there (see Section II).

the conical solution via a marching technique. The marching is

an artificial gimmick with which the conical solution, which

is, of course, independent of the radial coordinate, is obtained.

But in our problem, the blunted cone, the marching technique is

real! The blunt body solution generates physically meaningful

initial data for the conical afterbody solution. In the vicinity

of the nose there are neither singularities nor layers, as there

are in the pointed cone problem. So, when we couple the solutions

to the two unit problems, all the nastiness of the pointed cone at

an angle of attack disappears.

The second point concerns the formation of an entropy

layer far downstream of the nose region. One expects that the flow

over a blunted cone will approach grossly, at large distances

from the nose, that over a pointed cone, except, of course, for

the entropy near the cone surface. The description of this behavior

for large distances from the nose, really amounts to a mesh-size

problem. But it is not a trivial problem since every digital

computer has speed and storage limitations and we are already feel-

ing them. We are omitting any consideration of this sort of be-

havior at large distances, as this solution is meant to be a tool

to be used for relatively short bodies, probably on the order of

30 to 50 typical nose radii (or less) long.

THIS PAGE

WAS INTENTIONALLY

LEFT BLANK

16

THIS PAGE

WAS INTENTIONALLY

LEFT BLANK

In addition to the mesh size in the Φ direction (with $\Delta\Phi$ = constant = π/MACO, MACO an integer $\geq$ 2), it is necessary to divide the space between the shock and the cone into a number of strips, say NACO of them. For a given value of Φ, say Φ_m, the Θ mesh interval is set as

$$\Delta\Theta = \frac{\Theta_{shock} - \Theta_{cone}}{NACO} \quad .$$

Thus $\Delta\Theta$ varies with Φ. The resulting mesh on the R = constant = R_i surface looks like this (it is only necessary to consider $0 \leq \Phi \leq \pi$).

Φ=0

m=2

Φ, m increasing

Θ, n increasing

n=2

n=NACO + 2

Φ=π

m=MACO + 2

18
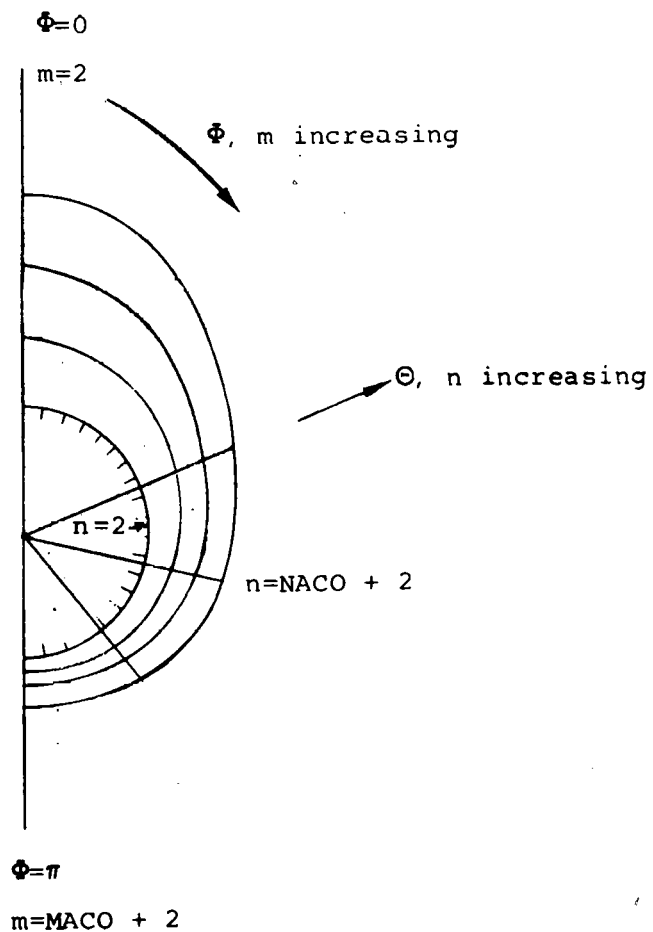
Now it is necessary to get the flow variables at each mesh point. Since we know (R, Θ, Φ) at each mesh point on the $R = R_i$ surface, the corresponding coordinate (r, θ, φ) in the blunt body solution can be computed directly. Then the blunt body flow field is searched to find the 'cube' in which the computed (r, θ, φ) are to be found. A simple linear interpolation between the given point and the data at the vertices of the cube then yields the flow variables at the point in question. The velocity components, of course, must also be transformed.

Now that the entire flow field on the constant R_i surface has been determined, it is necessary to be certain that it is supersonic everywhere. To this end a test is made at each point in the field, including the boundary points. If the flow is subsonic at a point (actually if $M^2 < 1.1$) we increase $R = R_i$ to $(R_i)_1 = 1.2(R_i)_o$ and repeat the above process.

While we are searching the blunt body solution for the points on the constant R surface, a check is made to be certain that the surface $R = R_i$ is not even partially outside the volume included in the blunt body solution. If it is, then there was not computed a large enough volume in the blunt body solution. The computation of that case is terminated and the data for the next case is read.

Suppose the initial data surface has been determined and the flow is everywhere sufficiently supersonic. It is then necessary to determine the shock derivatives on the $R = R_i$ surface, i.e., we must get

$$\left(\frac{\partial \Theta_{shock}(R,\Phi)}{\partial \Phi}\right)_{R = R_i} \quad ; \quad \left(\frac{\partial \Theta_{shock}(R,\Phi)}{\partial R}\right)_{R = R_i}$$

The term on the left is obtained from the known values of Θ_{shock} on the $R = R_i$ surface by a central difference. The term on the right is taken by finding the $\bar{\Phi}$ distribution of Θ_{shock} for $R = (1 + \epsilon_5)R_i$ and $R = (1 - \epsilon_5)R_i$, $\epsilon_5 \sim 0.05$. Then, a central difference of these values gives the desired term.

Now we have all the data necessary to make the computation of the flow about the conical afterbody. And that is what is done next.

C. Some Program Information

Finite difference mesh: In obtaining the blunt body solution it is necessary to specify a mesh, that is, to determine how many intervals are to be used in the r, θ, φ directions. A typical situation is to take five (5) intervals between the shock and the body, ten (10) intervals in the θ coordinate (for each

φ = constant plane), and about eight (8) meridional planes

(for $0 \leq \varphi \leq \pi$ since, because of symmetry, we need to

compute only half the nose region). For such a mesh,

approximately 6 minutes computing time are required on the

CDC 6600 digital computer. Now, the mesh to be used for the

cone solution should be of the same order of accuracy* as

that used for the blunt body program (e.g., 5 intervals in

the Θ direction, 6-10 intervals in the Φ direction for the

above case). Under these conditions the cone computation

will take considerably less time than that of the nose region.

Thus, in deciding what mesh size to use, one should direct

his efforts to the blunt body program, particularly if time is

a concern (the blunt body program is also more restricted due

to storage limitations).

The exceptional cases: Under certain circumstances

it may be impossible for the computer program to obtain the

complete solution. For instance, the blunt body solution may

not be completed because too small a region was specified and

the flow goes subsonic on part of the outer surface between the

---

* or higher; see the comments in Section IV.

shock and the body. Or, if an extremely rough mesh were specified, particularly at very high or very low Mach numbers, there may be numerical troubles. In such a case, the blunt body computation will fail somewhere. Then the program is instructed to print out an indication of the nature of the difficulty and, when possible, to proceed to the next case. Suggested remedies are to be found in the Appendix.

Shape of the nose: Currently the computer program is restricted to configurations which are either ellipsoids of revolution (including a sphere) or paraboloids of revolution, smoothly joined to the cone. The program cannot accept data specified pointwise.

Surface entropy: Moretti and Bleich assign to the body stream surface the entropy behind the steady normal shock, neglecting the fact that in the asymmetric case the streamline which wets the body surface generally is not the one which passes normally through the bow shock, but, rather, one near it.

D. Coordinate System Transformations

Here we put on record the formulae used to transfer data from the blunt body solution to the initial data surface for the conical afterbody solution.

In Figure 4 a schematic representation of the two principal coordinate systems is given. The (R,Θ,Φ) system is a body-oriented spherical polar system centered at the cone origin, O. The (r,θ,φ) system is a wind-oriented spherical polar frame centered at o, on the body axis a distance $L > 0$ from the cone apex. L must be large enough so that o is inside the body. The angle of attack is denoted by α.

Let $\bar{X}$, $\bar{Y}$, $\bar{Z}$ be a right handed Cartesian coordinate system centered at o with the $\bar{Z}$ axis aligned with the wind direction, the $\bar{X}\bar{Z}$ plane corresponding to pitch plane, $\bar{X}$ positive on the leeward side, and the $\bar{Y}$ axis in the $\bar{Z}\bar{X}$ direction, and let x_2, y_2, z_2, be a body-oriented Cartesian system centered at O, the cone apex, with the z_2 axis aligned with the body axis, the x_2 axis in the pitch plane, positive on the leeward side, and the y_2 axis in the $z_2 x_2$ direction. Furthermore, let the velocity components in each system be deonoted as follows:

Coordinate System	Velocity Components
R,Θ,Φ	u_o, v_o, w_o
r,θ,φ	u, v, w
$\bar{X}, \bar{Y}, \bar{Z}$	$\bar{U}, \bar{V}, \bar{W}$
x_2, y_2, z_2	u_2, v_2, w_2

Then, the transformation from the r, θ, φ (blunt body) system to the R, Θ, Φ (cone) system is given by:

1) $\begin{cases} x_2 = r(\sin\theta\cos\varphi\cos\alpha + \cos\theta\sin\alpha) \\ y_2 = r\sin\theta\sin\varphi \\ z_2 = r(-\sin\theta\cos\varphi\sin\alpha + \cos\theta\cos\alpha) + L \end{cases}$

2) $\begin{cases} R = \sqrt{x_2^2 + y_2^2 + z_2^2} \\ \\ \tan\Theta = \sqrt{x_2^2 + y_2^2}\,/z_2 \\ \\ \tan\Phi = y_2/x_2 \end{cases}$

3) $\begin{cases} \bar{u} = u\sin\theta\cos\varphi + v\cos\theta\cos\varphi - w\sin\varphi \\ \bar{v} = u\sin\theta\sin\varphi + v\cos\theta\sin\varphi + w\cos\varphi \\ \bar{w} = u\cos\theta - v\sin\theta \end{cases}$

4) $\begin{cases} u_2 = \bar{u}\cos\alpha + \bar{w}\sin\alpha \\ v_2 = \bar{v} \\ w_2 = -\bar{u}\sin\alpha + \bar{w}\cos\alpha \end{cases}$

5) $\begin{cases} u_o = u_2\sin\Theta\cos\Phi + v_2\sin\Theta\sin\Phi + w_2\cos\Theta \\ v_o = u_2\cos\Theta\cos\Phi + v_2\cos\Theta\sin\Phi - w_2\sin\Theta \\ w_o = -u_2\sin\Phi + v_2\cos\Phi \end{cases}$

To go from the R,Θ,Φ (cone) system to the r,θ,φ (blunt body) system, use the following formulae:

6)
$$\begin{cases} \bar{X} = R \sin \Theta \cos \Phi \cos \alpha - (R \cos \Theta - L) \sin \alpha \\ \bar{Y} = R \sin \Theta \sin \Phi \\ \bar{Z} = R \sin \Theta \cos \Phi \sin \alpha + (R \cos \Theta - L) \cos \alpha \end{cases}$$

7)
$$\begin{cases} r = \sqrt{\bar{X}^2 + \bar{Y}^2 + \bar{Z}^2} \\ \tan \theta = \sqrt{\bar{X}^2 + \bar{Y}^2}/\bar{Z} \\ \tan \varphi = \bar{Y}/\bar{X} \end{cases}$$

8)
$$\begin{cases} u_2 = u_o \sin \Theta \cos \Phi + v_o \cos \Theta \cos \Phi - w_o \sin \Phi \\ v_2 = u_o \sin \Theta \sin \Phi + v_o \cos \Theta \sin \Phi + w_o \cos \Phi \\ w_2 = u_o \cos \Theta - v_o \sin \Theta \end{cases}$$

9)
$$\begin{cases} \bar{U} = u_2 \cos \alpha - w_2 \sin \alpha \\ \bar{V} = v_2 \\ \bar{W} = u_2 \sin \alpha + w_2 \cos \alpha \end{cases}$$

10)
$$\begin{cases} u = \bar{U} \sin \theta \cos \varphi + \bar{V} \sin \theta \sin \varphi + \bar{W} \cos \theta \\ v = \bar{U} \cos \theta \cos \varphi + \bar{V} \cos \theta \sin \varphi - \bar{W} \sin \theta \\ w = - \bar{U} \sin \varphi + \bar{V} \cos \varphi \end{cases}$$

IV. <u>RESULTS AND DISCUSSION</u>

In this section we want to examine some results. The center of our attention is on the accuracy of the flow field calculations, not on the physical interest of the solution. Some effort to assess the accuracy is important if this is, in fact, to be a useful tool.

In our problem, the three-dimensional flow field for supersonic blunt nosed cones at an angle of attack, the solution is obtained by coupling a solution of the "blunt-body problem" with a solution of the "pointed-cone problem." Typical results for the separate solution of those two problems are given in References 1-4. Here, instead, we are primarily interested in the results of the coupling. Clearly the coupled solution depends not only on the attributes of the two unit problems, but also on how they have been joined. For instance, in obtaining initial data for the afterbody solution, it is necessary to do extensive interpolating on the blunt body solution. The accuracy of these interpolations depends, as we shall soon see, not only on how they are done but also where. And, of course, the solution of the afterbody flow field depends on the accuracy of this initial data. So we will pay particular attention to the manner in which this initial data is generated. The region which will show most

of these effects is on and immediately downstream of (say $\sim$ 20 nose radii or less) the cone initial data surface, and that is where our attention is focused.

A. Parameters, Introduced by the Numerics, into the Coupled Solution

The parameter, ϵ_6: In Section III.-B, we mentioned that the initial data surface must be at a value of $R_i \geq R_{MIN}$ where R_{MIN} is the value of R at which the sphere is attached to the cone. (Recall that (R, Θ, Φ) is a body-oriented spherical polar coordinate system centered at the cone apex.) In the vicinity of $R = R_{MIN}$ the body curvature changes very rapidly, as do, in general, the flow field variables. We might expect, therefore, that this would be a region in which interpolations on the blunt body mesh are at their worst. And, in fact, we expect the solution itself to be the least accurate in this region. Furthermore, the situation can be expected to improve rapidly as R_i is increased from R_{MIN} . Thus, in picking a value of $R_i \geq R_{MIN}$, we should expect that it would be wise to take $R_i = (1 + \epsilon_6)R_{MIN}$ where ϵ_6 is a positive constant which is bounded above by the fact that R_i must be small enough so that the initial data surface is included entirely inside the volume computed in the blunt-body solution. In addition, because of the extrapolations made in-the

blunt-body solution,[1,2,4] we should try not to get too close to the edge surface of the blunt body solution domain. So, we see that the choice of R_i is not to be made too lightly if you are interested in retaining as high a level of accuracy as is possible in the immediate vicinity of the initial data surface.

To get an idea of the effect of R_i on the inaccuracies due to linear interpolation, we consider the following case: a 1.5:1 ellipsoid attached to a 20° half-angle cone; Mach = 8; $\gamma = 1.4$; incidence = 15°; blunt body mesh has 5 x 10 x 8 intervals in r,θ,φ directions, respectively. Needless to say, the Θ component* of velocity (on the initial data surface) on the body surface should be zero for all $R_i \geq R_{MIN}$. In Figure 5 are plotted the maximum of the absolute value of this velocity component,

$$\frac{|v|_{max_{\Theta=cone\ \frac{1}{2}\ \sphericalangle}}}{U_\infty}$$

as a function of ϵ_6, where

$$R_i = (1 + \epsilon_6)R_{MIN}.$$

---

* R,Θ,Φ is the coordinate system centered at the cone apex

It is clear that you should take, for the mesh and body under consideration, $\epsilon_6 \geq \delta$ where $\delta \sim 0.05$.

The parameter ϵ_5: In preparing the data for the after-body solution, it is necessary to obtain the value of $(\partial\Theta_{shock}(R,\Phi)/\partial R)_{R=R_i}$. The most reasonable way to do this is to get $\Theta(R,\Phi)$ at $R = (1 \pm \epsilon_5)R_i$ and compute the partial derivative by central differences. The question is, what is the best value of ϵ_5 in order to get the derivatives as well as possible, or does it make much difference? The answer varies, of course, with Mach number, body shape, angle of attack, mesh size, etc., so it is impossible to give a comprehensive answer. However, let us look at Figure 6 where $\partial\Theta_{shock}/\partial R$ is plotted for several values of ϵ_5 and for $\epsilon_6 = 0.05$. The case is the same as in the preceding paragraph.

It is easy to see that there is significant scatter, though not surprisingly so. The maximum deviation is about 15% at $\Phi = 0^O$, (leeward plane) and 40% at $\Phi = 180^O$ (windward plane). Though this may at first sight seem like an intolerably large deviation, it really is not. Of course, you may go to a finer mesh if a higher degree of accuracy is desired. But there are limitations as far as computer storage and computing time are concerned, so we must seriously examine our present results to

see if they are acceptable. This is done at the end of this
section. As you will see, the results are very pleasing and
indicate that such variations in the initial shock slope
are quickly damped out and have insignificant effects on the
solution.

B. Comparison with Other Methods, at Least in
    Degenerate Cases

In order to compare our results we need something with
which to compare them. It would be nice if Babenko's cone
solution were attached to a blunt-body solution, but to our
knowledge this has not been done. So it seems that, unfortunately,
there is no other general three-dimensional flow field solution
available with which our results can be compared. So our compari-
son will be done on a problem which has axial symmetry.

For our comparison problem we will use a

spherically tipped $12\frac{1}{2}°$ cone,

free stream Mach = 6,

γ = 1.4,

zero incidence.

The results obtained using the solutions of Moretti and Bleich,[2,4]
and Moretti[3] will be compared with those obtained when the super-
sonic afterbody solution is computed by the method of character-
istics. We know that the method of characteristics is the most

accurate numerical method for integrating the Euler equations
for two-dimensional flow, and the same is true in most cases
where the flow is axisymmetric. So the comparison of the
Moretti technique with the characteristic computation will be
of value in determining, in particular, the mesh size necessary
for Moretti's technique to achieve the same accuracy obtained
by characteristics with a given mesh.

Seen in this generality, the comparison looks straight-
forward, and seems to sharply bring out just the difference
between the characteristic and finite difference marching solu-
tions. Things are, however, complicated by the following three
points.

We do not have exactly comparable blunt body computa-
tions, unfortunately, in the comparison. The current blunt body
solution is obtained using a spherical polar coordinate system
centered on the body (sketch A). The program available to us to
compute the supersonic flow by the method of characteristics
uses a different coordinate system, a quasi-cylindrical polar
one (sketch B).
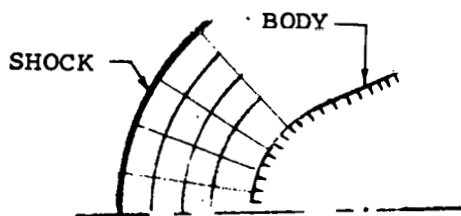
Sketch A

Finite difference grid for
spherical polar coordinate
system - current program
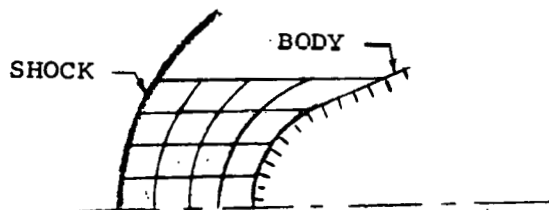
Sketch B

Finite difference grid for
quasi-cylindrical polar
coordinate system - afterbody
solution by method of character-
istics

In spite of this difference, the two grids are near enough
the same in the test case to consider their accuracy to be
essentially equivalent.*   Naturally, we expect the biggest dis-
agreement near or on the body where the cone attaches to the
spherical cap, i.e., in the region where the initial data is ob-
tained by interpolation. Clearly, without the same blunt-body
solution, we cannot have exactly the same initial data. Further-
more, the initial data for the characteristics solution is obtained
differently than is the initial surface data for the conical

---

*   c. f. Ref. 4 for a discussion of the merits of the polar frame,
    in particular with respect to highly blunt bodies and axi-
    symmetric bodies at an angle of attack.

afterbody solution. However, as you can see below, the pro-
cedure for generating initial data for the characteristics
solution is comparable to that being used in the coupling of
the three-dimensional solutions.

We ran the axisymmetric blunt-body program (Reference 1)
with the quasi-cylindrical coordinate system until the solu-
tion had settled down to a steady state. Then, in the
supersonic part of the flow field, a second family character-
istic was constructed from the shock to the body (see sketch).
This was done without averaging the characteristic slope
between mesh lines.
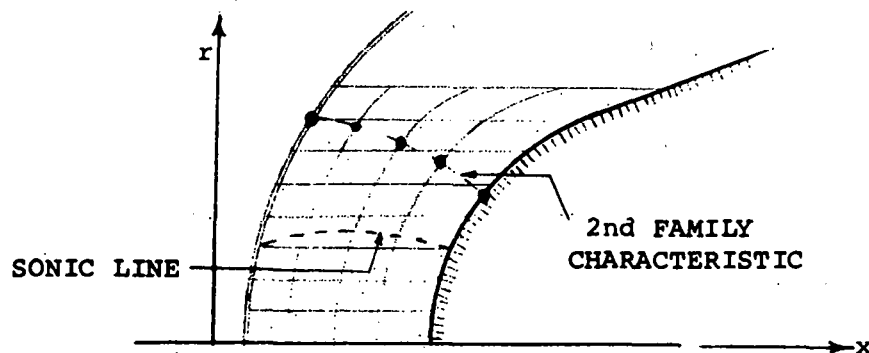
The data at mesh points on this initial 2nd family character-
istic are obtained by linear interpolation between adjacent

mesh points on the 'vertical' grid lines in the blunt-body

solution. Thus, if there are N mesh intervals in the x

direction in the blunt-body program, there will be N + 1

points on the initial characteristic. In order to refine

the characteristic mesh we divide each initial interval into

a number of subintervals. However, this is not all. There

is another difference which we record here for completeness,

even though it should not affect the comparison we are seeking.

The solution of the blunt-body problem was obtained using

the type of mesh shown on sketch B on page 32.   This mesh

has very poor definition near the attachment point (that is

one reason why the polar coordinate system was later adopted).

In addition, that computer program obtains the local body cur-

vature by differencing the local slopes. The result is that one

usually obtains wiggles in the shock shape due to nonsmooth data

prepared in a crude manner and to the idiosyncracies of the

coordinate system. It was found that these numerical difficulties

could be eliminated by smoothing the transition from the sphere

to the cone, i.e., by smoothing the curvature near the attachment

point. This was done by modifying the slope of the body as

indicated in the following sketch. Of course,

$$\frac{dx}{dr}$$

cot (cone 1/2 ∢)

—— original slope

— — — modified slope

r

r*
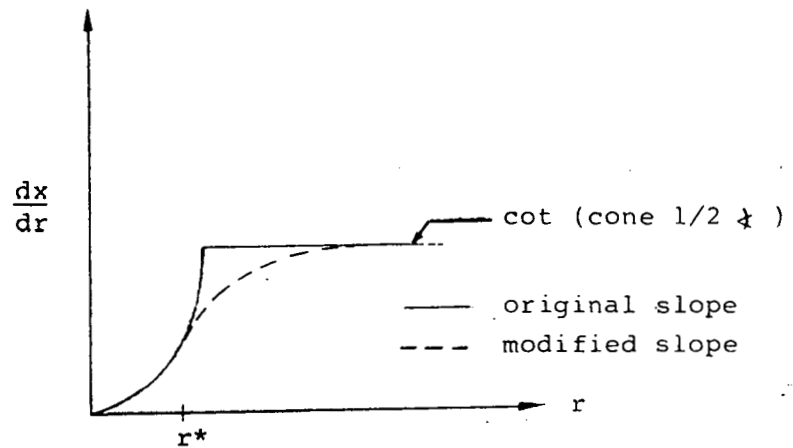
in order to be consistent it was necessary to then modify

x(r) for x > x* where the asterisk signifies the point at which

the smoothing is initiated. The result is a modified body as shown

in this sketch.

r

modified body

original body

x

x*
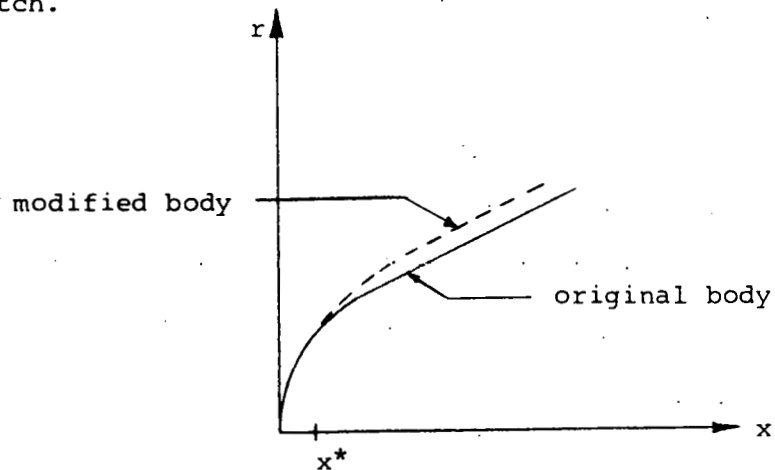
The modification to the body significantly alters the solution. The modified body introduces errors as high as 85% in the pressure and 19% in the Mach number, downstream of x*, in the comparison case. It was found that this method of modifying the body gave very good results on the unmodified part. This was particularly the case when x* was somewhat downstream of the sonic point on the body.

If x* is even downstream of the limiting characteristic, in the steady case the modification has no influence on the subsonic part. This is true for the exact analytical solution. It is expected to be well satisfied also for the steady numerical solution which is built up with the unsteady technique. In the current check case, x* is, in fact, downstream of the limiting characteristic so, in the steady case, it should have no influence on the subsonic part. x* is also downstream of the initial characteristic and thus, by returning to the unmodified body in the characteristic computation, we are able to make the complete solution without the influence of the modified body, since the characteristics solution recomputes the region affected by the modified part of the body.

As a by-product of the comparison we can also very nicely see what the effect of the smoothing was. And, finally, we have a good way of evaluating the accuracy of the polar coordinate system blunt-body program which does not have any sort of smoothing but which does give pretty good definition near the attachment point. A last point on how we set up the comparison; remember that the characteristic mesh is not fixed, so we will characterize the characteristic mesh size by its value on the initial data line generated by the blunt-body solution.

A note of comfort is certainly in order. There are, of course, many little difficulties in setting up this comparison. But, the results can be read and the comparison made. To be fair we must have comparable mesh sizes and a proper reading of the results.

So here is how we chose the mesh sizes for the two blunt-body solutions, the quasi-cylindrical coordinate system first. The blunt body mesh size we have used is constant in the vertical direction, $\frac{\Delta r}{r_n} = \frac{1}{5} = 0.2$ where r_n is the radius of the sphere. There are 5 mesh intervals between the shock and the body. We took a total of 6 intervals in the r direction so that the maximum ordinate is $r_{max}/r_n = 1.20$. The results of this program will be labeled BBCMOC (Blunt Body Cylindrical-Method of Characteristics).

Now let's look at the setup for the current program. In this case the blunt body solution is obtained in a spherical polar coordinate system. The coordinate system was centered on the body axis at $x = 0.5$ r_n downstream of the center of the sphere. We took a mesh of 5 intervals in the radial direction and 10 intervals in the θ direction, with $\Delta\theta = 9^0 = .15708$ rad. This gives a typical mesh spacing on the body of $\frac{s}{r_n} = (1+.5)\Delta\theta = 0.236$ in the θ direction. There are the same number of intervals between the shock and the body in the two cases. So we can consider the two cases run with the two programs to have essentially comparable mesh sizes. The results of this program, the current one, will be labeled BBPMAB (Blunt Body Polar-Moretti Afterbody).

In this comparison we have not refined the blunt body mesh but have concentrated our attentions on the afterbody flow field solutions.

Now let's look at the comparison between the current afterbody flow field solution and the method of characteristics for axisymmetric flow. In making the comparison we will concentrate our attention on four areas:

i) the body surface near the attachment point;

ii)   the body surface further downstream;

iii)   the bow shock wave near the initial data surface;

iv)   the shock wave further downstream.

First we will consider the effect of mesh size on i) - iv).

i)   <u>The body surface near the attachment point</u>.

This is the region in which the streamlines have their

maximum curvature and where things change the most rapidly

(except, of course, across the shock wave). So this will be a

particularly good check of the current solution. The compari-

sons are shown in Figures 7 and 8. In order to read the

figures, remember that the two programs are referred to as

BBPMAB (current technique) and BBCMOC (comparison problem). It

is clear that:

the blunt-body solution using the polar

coordinate system (current program) gives

very accurate results, even in the immediate

vicinity of the attachment point. In fact,

the blunt body solution (polar coordinate

system) disagrees by only a maximum of 3% in

the Mach number and 2-3% in the pressure with

the characteristic solution which has five

times as many points between the shock and

the body.

ii) <u>The body surface further downstream</u>.

The purpose of this comparison is to get an idea of the

accuracy of the computation on the cone using the technique

of Moretti[3]. We will pay particular attention to the effect of

the number of mesh intervals between the shock and the body,

keeping in mind the following two points:

a) there are quite large pressure gradients

between the shock and the body immediately

downstream of the attachment point,

b) further downstream the entropy layer

begins to form near the cone surface.

The current program was compared against two character-

istic computations, one having five and the other twenty-five

mesh intervals on each right running characteristic. The

BBPMAB program was run with the cone solution obtained with 5,

10 and 20 intervals between the shock and the body. In all the

following cases, $\epsilon_5 = 0.04$ and $\epsilon_6 = 0.10$. The results are

presented in Figures 9 and 10 where it can be seen that the 10-

interval mesh agrees quite well with the solution of the

20-interval mesh. The Mach number and pressure distribution

for those two meshes agree to within 2% of the characteristics

solution.

iii) <u>The bow shock wave near the initial data surface</u>.

Figures 11 and 12 give the shock shape and static pressure

immediately behind the shock for the five runs we have been

discussing. As might be expected, the agreement between the

two techniques is even better than it was on the body. This

is also true for

iv) <u>the bow shock wave further downstream</u>, as can be

observed in Figures 13 and 14.

C. <u>Further Results on the Effect of ϵ_6 and ϵ_5</u>

We have seen that we can have quite large inter-

polation errors when ϵ_6 is small. In order to see how these

interpolation errors affect the solution downstream, we have

obtained solutions to the current program with $\epsilon_6 = 0$ and

$\epsilon_6 = 0.1$. The blunt body mesh was the same as before, and we

have taken 10 intervals between the shock and the body in the

cone program and $\epsilon_5 = 0.04$. The results are shown in Figures

15-17. Note, in particular, the drifting of the pressure

behind the shock in the region $6 < R/r_n < 14$. This is a result

of interpolation inaccuracies, but in the interior field, not

at the body! This was seen by noting that the left running

characteristics that intersect the shock in the vicinity

$R \sim 6$ originate, not at the body, but in the interior of the

initial data surface where the change in the pressure gradient

$(\partial p/\partial \Theta)_{R=R_i}$ is a maximum. The maximum drifting in pressure

behind the shock is about $2\frac{1}{2}\%$ and in shock angle is about 0.5%.

These effects of interpolations on the initial data surface

can be reduced, if it is necessary, by taking a finer mesh in

the blunt body and the cone programs. It just costs money!

We also have varied ϵ_5 keeping $\epsilon_6 = 0.0 = $ constant.

The results of the same case for $\epsilon_5 = 0.04$ and 0.08 are shown

in Figures 18 and 19 where it can be seen that the rather

large discrepancies (20%) in $(\partial \Theta_{shock}/\partial R)_{R=R_i}$ as computed for

the two values of ϵ_5 die out quite quickly. At $R = 4.74$

where the shock derivatives agree to within 0.07%, the shock

angles agree to within .15%.

Finally, remember that the accuracy we are talking

about is for the solution of three-dimensional flow fields!

D. Conclusion

From the results presented it is clear that this

synthesis offers a very useful means of obtaining three-

dimensional inviscid flow field solutions about blunt axi-

symmetric cones at an angle of attack. The solutions are
accurate, easy to obtain (see the Appendix) and inexpensive,
particularly considering the accuracy attainable.

V.   APPENDIX - PROGRAM USER's MANUAL

A.   How to Use the Program

This appendix is dedicated to the user and is devoted to the proposition that every potential user of the program ought to have, without going through too much discomfort, the answers to the following questions:

a.   What does the program do?

b.   What are the assumptions, restrictions, and limitations?

c.   What are the data required by physics?

d.   Are additional or redundant data required to make the program work?

e.   What form does the data take in the program?

f.   What will I get in return (i.e., what are the outputs)?

g.   How do I read the output?

h.   What might go wrong? What can I do about it?

i.   How much must I pay to get the results I need?

j.   What else can you tell me to minimize my discomfort?

In certain instances we will refer to previous discussions in order not to be redundant. In section B a

detailed outline of the input-output formats is given.

1. Questions and Answers

    a. <u>What does the program do</u>? It computes inviscid flow field about a blunted right circular cone at an angle of attack.

    b. <u>What are the assumptions, restrictions and limitations</u>?

body:	axisymmetric
	blunted nose followed by a right circular cone – the blunted nose is either a sphere, ellipsoid, or paraboloid of revolution
	continuous slope
gas:	inviscid $(\mu = 0)$; Euler equations
	uniform, constant specific heat ratio, thermally and calorically perfect
aerodynamic:	body flight speed is steady and sufficiently supersonic so that the subsonic flow is limited to the nose region
	angle of attack

In addition, the restriction on the distance downstream of the nose region (as noted in III) should be noted. See also the comments on the body stream surface entropy distribution in the same section.

c. <u>What are the data required by physics?</u>

The physical problem, under the above limitations,

requires the following data:

body geometry (including β, the cone

semi-angle)

γ,   the specific heat ratio

M_∞,   the free stream Mach number

α,   the angle of attack

d. <u>Is additional or redundant information</u>

<u>required to make the program work?</u>

Additional – yes.

Redundant – no!

In addition to that indicated under (c), it is

necessary to supply the following data:

i. a title card of up to 72 alphanumeric
    characters (may be left blank, but not
    left out)

ii. the date and run number (optional)

iii. certain integers fixing the mesh in each
    program

iv. integers fixing the number of time steps
    in the blunt body program and the maxi-
    mum number of radial steps in the cone
    program

    v.   integers controlling output

   vi.   iteration tolerances and ϵ_5 and ϵ_6
          (see III-A)

  vii.   the maximum distance downstream to
          be computed in the cone program

 viii.   stability coefficients

   ix.   maximum θ coordinate in blunt-body pro-
          gram

    x.   position of coordinate system origin for
          blunt-body program

A step-by-step journey through the data cards is

given in part B of this Appendix.

    e. <u>What form does the data take in the pro-</u>

<u>gram?</u> All data are read from standard IBM cards.

The characters are alphanumeric. Integers are

read with I formats, floating point numbers with

E formats.

    f. <u>What will I get in return (what are the</u>

<u>outputs)</u>? At the beginning of each case, all in-

put data are printed out. Then the initially

assumed flow field for the blunt-body program is

written. At the end of the blunt-body computation,

the entire flow field in the nose region is printed.

The blunt-body solution is given in <u>both wind-and</u> <u>body-oriented spherical</u> polar coordinate systems. (If desired, it is possible to get output at intermediate times also.) Then the data on the initial data surface for the cone program is printed. During the subsequent computation of the flow field about the conical afterbody, you may printout as often as desired, including every step. There are no provisions to print-out at specified times in the blunt-body program or specified stations in the cone program. All output is controlled by step counters.

All reading and printing is done with standard FORTRAN 4 statements. The input tape is logical tape 5, the output tape is logical tape 6. No other tapes are required or used (other than standard system tapes).

g. <u>How do I read the output?</u> For step-by-step journey, see part C of the Appendix. In part B, INPUT, of the Appendix, a complete list of the input parameters, including their FORTRAN

symbols and, where appropriate, recommended values, are given. The first pages of the output contain the input data, and there should be little difficulty in interpreting this information.

The following pages give the geometry data in the wind-oriented polar spherical frame, for each mesh point on the body surface. The data is presented in groupings which correspond to different meridional planes in the wind axes system. In the report, meridional planes are planes referred to the coordinate systems and do not necessarily mean body meridional planes. Thus, in the (r, θ, φ) wind-oriented system, planes of constant φ are referred to as meridional planes, though they are not meridional planes of the body. The value of $\theta = 0$ corresponds to the direction "into the wind."

The next output is the initial data for the blunt-body program. This is essentially arbitrary and is printed out more for completeness than any other reason. Do not try to give this data a physical significance. The meaning of most of the

symbols should be evident (see section C). Then
there may be a number of outputs of the unsteady
blunt body computation, if the user so specifies.
When the blunt body computation is finished, the
final steady state values will be printed out.
Then the coordinate system transformation is made
to find the initial data for the cone program.
Subsequently, this initial data is printed out
followed by the output of the solution at various
constant R surfaces downstream of the initial
data surface. When the computation has exceeded
the maximum value of R (an input) to be computed,
or if the maximum number of steps in the R direction
is exceeded, the flow variables at the last step
are printed out and the next case is begun (if
there is another).

h. What might go wrong? What can I do
about it? There are basically only two problems
that may arise (so long as the proper data is
input). The first is that there may be
failures in iterations at boundary points in

either program. In such a case, usually the difficulty is that either the mesh is too rough for the case considered, or the flow in the blunt-body solution has become subsonic on the outer surface between the shock and the body. In the former case, _increasing the number of mesh points_ is the solution; in the latter case it is necessary to _increase the size of the domain being computed_.

A second type of problem is that the blunt-body solution domain is not large enough to allow the determination of an initial data surface for the cone program (see section III-C). In this case, it is again necessary to increase the size of the domain being computed by the blunt-body program.

i. _How much must I pay to get the results I need?_ Of course, the answer to this question depends on many variables, including the computer being used, the rate at which computer time is charged, and the accuracy required. We

will supply the information needed to make a
fairly good computation of time requirements, and
the rest is up to you.

Consider a 2:1 ellipsoid with the major axis
inclined 15° to the normal to the free stream
direction. Let the ellipsoid be followed by a 20°
half-angle right circular cone. Taking a mesh of
5 by 10 by 8 intervals (in the r, θ, φ directions,
respectively) for the blunt-body solution, the
computing time to go 300 time steps, including
program compilation, is about 5 minutes on the
CDC 6600. The conical afterbody flow field com-
putation is an order of magnitude faster for
comparable mesh size and will not be considered
here. Usually, 300-600 time steps are sufficient
to reach a satisfactory level of steadiness for
this degree of mesh fineness. The required time
decreases somewhat as the Mach number increases
and as the mesh size increases.

Note that if one halves the mesh interval
in each direction, the computing time will be

increased roughly by a factor of 2^4, not 2^3. The additional factor comes in because the maximum permissible time step is determined by a stability criterion which is a linear function of the mesh intervals. Since the important parameter in reaching a level of steadiness is elapsed time (not the number of steps), a decrease in the time step leads to more steps to reach a given time.

j.   What else should I know when using this program? Currently the program occupies about 106,000 octal locations on the CDC 6600 digital computer. The maximum number of mesh intervals are:

blunt body   (5x10x9) in (r,θ,φ) directions,

conical afterbody (30x18) in (Θ,Φ) directions.

Remember, there is no automatic test to determine when the blunt body solution has reached a specified level of steadiness. You must specify the number of time steps to be computed.

B.   Input

This section on program input is divided into three parts: general comments, a list of the input with complete

instructions on how to prepare it, and a sample case with appropriate comments.

    1.   <u>General Comments</u>

        There are a number of things to be discussed here and they come under two subheadings; problem-oriented and program-oriented comments.

        a.   <u>Problem-oriented comments</u>

            i)   <u>Data to be specified</u> – A minimum amount of data is required from the physical point of view. They are:

                free stream Mach number,

                ratio of specific heats,

                body geometry, suitably scaled.

        Note that you need not, in fact are not allowed to, pick reference conditions.

        ii)   <u>Geometry of the nose region</u> – As previously mentioned, the blunt nose can either be an ellipsoid of revolution (including a sphere as a special case) or a paraboloid of revolution. The nose is followed by a right circular cone which merges smoothly with the nose configuration (Figure 3).

b.   Program-oriented comments

    i)   Nondimensionalization and scaling –
The nondimensionalization has been fixed in the pro-
gram, and you do not have the choice of specifying
reference quantities. The free stream pressure,
density, and entropy have been chosen as reference
quantities, along with a length. If the nose is an
ellipsoid (sphere), the reference length is the semi-
axis "normal" to the free stream. If the nose is a
paraboloid, it is one-half the semi-latus rectum
(one-half the distance from the focal point to the
vertex). In summary, let γ be the ratio of specific
heats. Then the nondimensionalization is:

lengths are divided by			ℓ_0 (ℓ_0 is the reference length)
pressures	"	"	"	p_∞
densities	"	"	"	ρ_∞
velocities	"	"	"	$\sqrt{\gamma p_\infty / \rho_\infty}$
times	"	"	"	$\ell_0 / \sqrt{p_\infty / \rho_\infty}$
entropies $(S-S_\infty)$	"	"	"	c_v

ii) Stability coefficients - The
numerical analysis results in the solution being
obtained by a conditionally stable explicit finite
difference scheme. The integration step size must
be kept below some maximum value which cannot be
explicitly determined due to the nonlinearity of
the problem. An estimate of the upper bound is
obtained from the linearized equations and that
estimate is used to determine the maximum step size
allowed by the program. In order to provide for a
little flexibility in this direction, you also have
the option of multiplying the computed step size
limit by a factor which will further limit (if the
factor < 1) the step size. It is recommended that
this factor be taken as unity, meaning that the
linear limit is used.

iii) Coordinate system origin location -
In using this program there are good reasons (see
Sections II, III and References 1 and 4) for taking
care in specifying the domain to be computed by
the blunt body program. For this reason, not only
do you have the pleasure (and duty) of specifying

the maximum value of θ for each φ = constant plane (it is the same for each plane), you also must specify the location of the coordinate system origin. This is done by specifying the value of a parameter, XO, which is the distance from the ellipsoid (sphere) center or paraboloid focal point to the coordinate system origin, measured positive "in the free stream flow direction." When XO $\neq$ 0 it is imperative that it be nondimensionalized in the manner indicated in (i).

The coordinate system origin for the cone program is located at the cone apex.

iv) <u>Coordinate systems</u> - There are a number of comments to be made which ought to clear up any doubts about what coordinate systems are used and where the axes are located. These comments are only concerned with the information necessary for the use of the program. Thus, we will discuss two coordinate systems.

<u>Blunt body program</u> - The solution of the blunt body region is obtained in a wind

oriented spherical polar coordinate system centered on the body symmetry axis. The reasons for using a wind-oriented system are given in Reference 4 and will not be gone into here. Of course, a wind-oriented system is not the most convenient from the standpoint of the person who uses the program. So provisions have been made to write all output in a body-oriented spherical polar coordinate system centered at the cone apex. Note, however, that in the body-oriented system the mesh points are not given on a number of meridional planes, and the spacing in the Θ and Φ directions is not constant.

In the wind-oriented system, for output purposes only, the $\theta = 0$ direction is taken to be positive into the wind. $\varphi = 0$ is in the pitch plane on the leeward side. φ is positive increasing in the counter clockwise direction when facing into the wind.

Note that the program actually works with a wind-oriented system with $\theta = 0$ in the downstream

direction, and the transformation equations given in Section III-D have $\theta = 0$ and $\Theta = 0$ in the downstream direction. However, for your convenience, the wind-oriented blunt body output is referred to a system with $\theta = 0$ upstream.

The body-oriented system is the same as that for the cone program which follows.

Cone Program - The conical afterbody solution is referred to a body-oriented, spherical polar coordinate system centered at the cone apex (if the cone were sharp). The $\Theta = 0$ direction is along the body axis in the downstream direction. Thus, the cone surface is given by $\Theta =$ constant $= \beta$, the cone semi-angle. $\Phi = 0$ is the leeward side of the pitch plane, $\Phi = \pi$ is the windward side of the pitch plane. Φ is positive increasing in the counter clockwise direction when facing into the wind.

v) Mesh size - Since the solution is obtained by a finite difference method over a grid defined by a number of points, it is necessary to specify the number of mesh points (actually mesh

intervals are specified) to be used in each coordinate direction. The decision is, as usual, one in which a compromise between accuracy and cost has to be made. Fortunately, the program gives quite good results even with a rough mesh. Consistency in accuracy should be maintained when picking the mesh for the blunt body and the after-body computations. In addition, the comments (Sections III, IV) relating to the size of the region to be computed should receive due consideration.

2.   Input List and how to Prepare the Input

The data for each case consists of six data cards. There is no flexibility in this number. It can be neither greater nor less than six.

On all the cards, except the first, the first seventy (70) columns are used (not all will have entries, though). 71 and 72 may be used on the first card. All integers are read with an I5 format and must be right adjusted. All floating point numbers are read with an E10.4 format.

Floating numbers having explicitly specified
exponents must be right adjusted. In addition,
there is a title card which is read with an A
format. The input tape is logical tape 5. The
output tape is logical tape 6. The data, card
by card, are as follows. (The capitalized sym-
bols are the program FORTRAN symbols used for the
variables in question.)

Card #1 - This is a title card. Any title com-
posed of alphanumeric symbols may be
entered in Cols. 1-72. The data are
read with a 12A6 format and are immedi-
ately written out.

Card #2 - This card has only integers. They must
all be right adjusted.

Cols. 1-5   NRUN   are for the run number;
you may enter any
integer of 5 or
fewer digits.

Cols. 6-10   MONTH   are for the number

                        of the month (May =

                        05) (two digits only)

Cols. 11-15   MDAY   are for the day of the

                        month (two digits

                        only)

Cols. 16-20   MYEAR   are for the last two

                        digits of the year

                        (two digits only)

The following data on this card all refer to

the blunt body program.

Cols. 21-25   NA   contain the number of

                        mesh intervals in the

                        r direction (maximum

                        of 5).

Cols. 26-30   MA   contain the number of

                        mesh intervals in the

                        θ direction (maximum

                        of 10).

Cols. 31-35   LA   contain the number of

                        mesh intervals in the

φ direction (maximum of $\underline{9}$).

Cols. 36-40	KA	contain the number of time steps to be taken in the blunt body program.
Cols. 41-45	JA	contain the output control for the blunt body program. The time-dependent solution will be written out every JA time steps.
Cols. 46-50	LB	contain the partial output control. If LB = 0, there is no partial output. If LB $\neq$ 0, the partial output will be written at every time step. The partial output consists of items

Cols. 51-55   LE   listed in Section C of this appendix. contain the nose geometry code. If LE = 1, the nose is an ellipsoid (spheroid) of revolution. If LE = 2, the nose is a paraboloid of revolution. LE must be either 1 or 2.

Card #3 - This card contains five pieces of data, the first three of which are iteration tolerances.

The tolerances are relative tolerances, and a suggested value is 10^{-4}. There is ordinarily no need to have a tighter tolerance.

Cols. 1-10   EPS(1)   Tolerance for iteration in shock computation in blunt body solution (10^{-4}).

Cols. 11-20   EPS(2)   Tolerance for iteration in body

64

computation in blunt body solution (10^{-4}).

Cols. 21-30   EPS(3)   Tolerance for iteration in shock and body computation in cone solution (10^{-4}).

Cols. 31-40   EPS(4)   This datum is not used.

Cols. 41-50   EPS(5)   In computing

$$\left(\partial \Theta_{shock} / \partial R \right)_{R=R_i}$$

for the initial surface, the shock shape for

$$R = [1 \pm EPS(5)] \cdot R_i$$

is computed and $\partial \Theta / \partial R$ obtained by central difference. Recommended value for EPS(5) is from 0.02 to 0.05.

Cols. 51-60 EPS(6) $(R_i)_{min}$ is the value of
R at the intersection of
cone with the blunt nose.
If $R_i = (R_i)_{min}$ is taken,
interpolation on the
body will be poor due
to the curvature of the
nose region. Hence,
for initial R we take
$R_i = [1 + EPS(6)](R_i)_{min}.$
Recommended value ~ 0.1.

Cols. 61-70 EPS(7) This datum is not used.

Card #4 – This card and the first two data on Card #5
contain the physical flow field data, body
nose information, and coordinate system
location.

Cols. 1-10 ACH M_∞, the free stream Mach
number.

Cols. 11-20 GAMMA the specific heat ratio,
$\gamma = c_p/c_v$.

Cols. 21-30   STAB   stability coefficient

for the blunt body

computation; recom-

mended value = 1.0

Cols. 31-40   THEMAX θ_{max}; in the blunt body

solution, the maximum

value of θ, in degrees,

to be used, where θ is

zero into the wind in

the wind axis system.
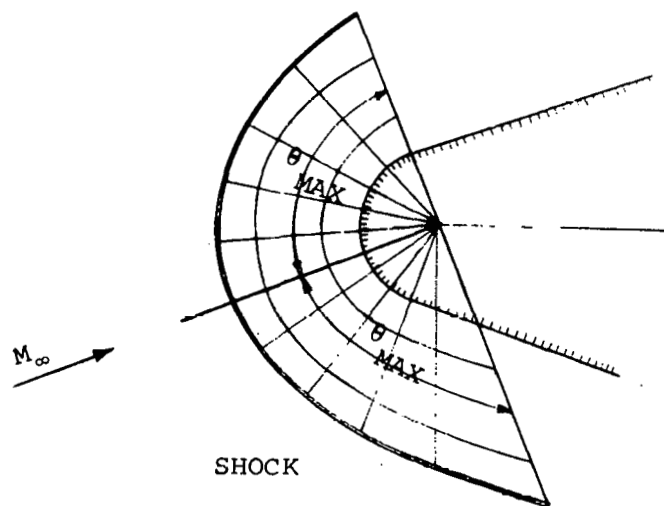
Cols. 41-50 **ELL**   Axis ratio if the body

is an ellipse.

$$\frac{1}{\text{ELL}}$$

1.0
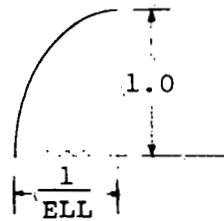
Cols. 51-60 XO   Distance from para-

bola focal point or

ellipse center to the

coordinate system

center measured positive

"downstream". (See

Appendix-B-1-b-i).

1.0

X_o

ellipse
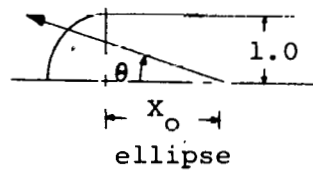
Cols. 61-70 ANGLE β, the half angle of the

conical afterbody

(degrees)
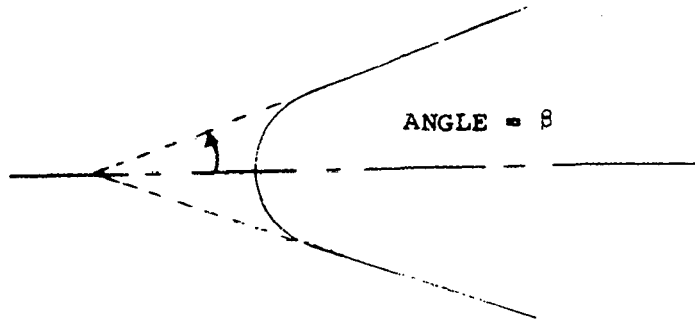
ANGLE = β

Card #5 - Cols. 1-10   ALPHA α, the angle of attack

in degrees (must be

$\geq$ 0).

Cols. 11-20 STABCO   the stability coeffi-

cient in the cone

solution; recommended

value = 1.0.

Cols. 21-30 RTMAX   the maximum value of R

to be computed in the.

cone program. See

Appendix -B-1-b-i and

Section III.

Card #6 - This card contains the control integers and
mesh specification for the conical afterbody
program. Do not forget that the integers
must be right adjusted.

Cols. 1-5   NACO   the number of Θ mesh

intervals

(maximum of 30).

Cols. 6-10   MACO   the number of mesh

intervals in the Φ

direction for

$0 \leq \Phi \leq \pi$ (maximum

of 18).

Cols. 11-15   KACO   the maximum number of

steps to be taken by

the conical afterbody

program.

Cols. 16-20   JACO   output every JACO steps

in the cone program.

And that completes the input data. Remember,
all integers are read with an I5 format and all
floating point numbers with an E10.4 format.

Floating point numbers with exponents and integers must be right adjusted.

A schematic input table is on the following pages.

Sample data are given in the next section.

SHORT SUMMARIZATION TABLE OF INPUTS

CARD NO.	COLUMNS	FORMAT	FORTRAN SYMBOL
1	1-72	12A6	(TITLE CARD)
2	1-5	I5	NRUN
	6-10		MONTH
	11-15		MDAY
	16-20		MYEAR
	21-25		NA
	26-30		MA
	31-35		LA
	36-40		KA
	41-45		JA
	46-50		LB
	51-55		LE
3	1-10	E10.4	EPS(1)
	11-20		EPS(2)
	21-30		EPS(3)
	31-40		EPS(4)
			(Not used by program)
	41-50		EPS(5)
	51-60		EPS(6)

CARD NO.	COLUMNS	FORMAT	FORTRAN SYMBOL
3	61-70		EPS(7)
			(Not used by program)
4	1-10	E10.4	ACH
	11-20		GAMMA
	21-30		STAB
			(1.0 recommended)
	31-40		THEMAX
	41-50		ELL
	51-60		XO
	61-70		ANGLE
5	1-10	E10.4	ALPHA
	11-20		STABCO
			(1.0 recommended)
	21-30		RTMAX
6	1-5	I5	NACO
	6-10		MACO
	11-15		KACO
	16-20		JACO

c.   Sample Input with comments

Following are the data for a twenty-degree half-angle cone tipped by a 1.5:1 ellipsoid of revolution with the major axis against the wind. The angle of attack is 20°. The physical data are:

1.5:1 ellipsoid followed by 20° half angle cone

M_m = 8

γ = 1.4

α = 20°

Card #1 - This is a title card giving the desired information.

Card #2 - The run number is 1 , (NRUN = 1), the date is 6/18/68 (MONTH = 6 MDAY = 18, MYEAR = 68). In the blunt-body program there are 5 mesh intervals between the shock and the body (NA = 5), 10 intervals in the θ direction for each meridional plane (MA = 10), and 8 meridional intervals (LA = 8). The number of time steps to be taken are 300 (KA = 300), the solution is to be output every 300 steps

(JA = 300), no partial outputs are de-
sired (LB = 0), and the nose is an
ellipsoid (LE = 1).

Card #3 - The iteration tolerances are all 10^{-4}
(EPS(1) through EPS(3) = 1.E-4); the
spacing of the R = constant planes from
which $(\partial\Theta_{shock}/\partial R)_{R=R_i}$ to be computed is
$\Delta r = 0.04R$; (EPS(5) = 0.02); and the
initial data surface is at $R_i = 1.1(R)_{min}$
(EPS(6) = 0.1)

Card #4 - $M_\infty = 8.0$ (ACH = 8.0); $\gamma = 1.4$ (GAMMA =
1.4); blunt body stability coefficient
= 1.0 (STAB = 1.0); maximum $\theta = 90^\circ$ for
each meridional plane in the blunt body
solution (THEMAX = 90.0); the nose is a
1.5:1 ellipsoid, major axis "vertical"
(ELL = 1.5); the blunt body coordinate
system center is located on the body axis
at a distance of 0.5 major semi-axes down-
stream of the ellipsoid center (XO = 0.5);
the afterbody is a 20° half-angle cone
(ANGLE = 20.0).

Card #5 - The angle of attack is 15° (ALPHA = 15°);
the stability coefficient for the cone
program is unity (STABC$\overline{\text{O}}$ = 1.0); compute
a maximum of 20 major semi-axes down-
stream in the conical afterbody solution
(RTMAX = 16.0).

Card #6 - In the conical afterbody solution there are
10 mesh intervals between the shock and
the body (NACO = 10); ten mesh intervals
in the Φ coordinate (MACO = 10); a max-
imum of 20 axial steps are to be taken
(KACO = 20); and output is to be given
every 2 axial steps (JACO = 2).

A picture of the actual data cards is shown on
the following page. Sample output and a discussion
thereof is given in the following section.

```
1.5 TO 1 ELLIPSE- 20 DEG. CONE, XO=.5,ALPHA=15   S DECK                    1
  WORD 1    WORD 2    WORD 3    WORD 4    WORD 5    WORD 6    WORD 7    WORD 8

     1   6     18  68     5  10     8  300    300   0     1                2
  WORD 1    WORD 2    WORD 3    WORD 4    WORD 5    WORD 6    WORD 7    WORD 8

   1.E-4     1.E-4     1.E-4      .02       .1                             3
  WORD 1    WORD 2    WORD 3    WORD 4    WORD 5    WORD 6    WORD 7    WORD 8

 3.0       1.4       1.0       90.       1.5       .5        20.           4
  WORD 1    WORD 2    WORD 3    WORD 4    WORD 5    WORD 6    WORD 7    WORD 8

 15.       1.0       16.0                                                  5
  WORD 1    WORD 2    WORD 3    WORD 4    WORD 5    WORD 6    WORD 7    WORD 8

   10  10    20   2                                                       6
  WORD 1    WORD 2    WORD 3    WORD 4    WORD 5    WORD 6    WORD 7    WORD 8
```

SAMPLE DATA

C.   Output

1.   Description of Sample Output

In this Section we discuss the output.
In part b) of this section, sample output
corresponding to the sample input given in the
preceding section are presented. We will not
spend extra time on explaining those items which
should by now be evident. For instance, the
first page of output should be pretty clear in
that it is just the input data with the appro-
priate notation.

The set of data following the first page
give the body geometry data for each wind-ori-
ented meridional plane in the blunt body system.
This data is computed analytically. The coor-
dinate system (r, θ, φ) is, of course, the wind-
oriented one centered on the body axis a dis-
tance XO (semi-major axes) downstream of the
body center. The data is in groups correspond-
ing to a constant value of φ, beginning with
$\varphi = 0^{\circ}$ (leeward pitch plane) and ending with
$\varphi = 180^{\circ}$ (windward pitch plane). Intermediate

planes are at intervals $\Delta\varphi = 180°/LA$. L is a
running index for φ, and L=2 at $\varphi = 0°$. For
each value of φ, the data is given as a function
of θ at intervals $\Delta\theta = \theta_{max}/MA = THEMAX/MA$.
$\theta = 0$ is the wind axis, pointing into the wind.
The parameter M is a running index for θ, and
M = 2 at $\theta = 0$. Thus $\theta = (M - 2)\Delta\theta$. The
columns, from left to right, are, for given φ:
M, θ, r, $\partial r/\partial\theta$, $\partial^2 r/\partial\theta^2$, $\partial r/\partial\varphi$, $\partial^2 r/\partial\varphi^2$,
$\partial^2 r/\partial\theta\partial\varphi$. Following the body data output, we
write the initial flow field data assumed for
the blunt body solution. Do not attempt to
attach a physical meaning to this data, it has
none.

At the top of the page the step number,
the nondimensional time, the three indices
identifying the mesh point which governs the
stability step size, and the step size are
written. Subsequently the flow field data for
each wind-oriented meridional plane is written.

First, the plane number, L, and the meridional
angle, φ, are printed. These are followed by the data
of the shock in that meridional plane, namely r_{shock},
$\partial r_{shock}/\partial t$, $\partial r_{shock}/\partial \theta$ as functions of θ for given φ.

Now, recall the manner in which the flow field
is partitioned into a mesh and you will realize that
in a meridional plane the mesh looks like this

Mesh for given meridional plane L,
where $\varphi = (\ell-2)\dfrac{\pi}{LA}$ in radians
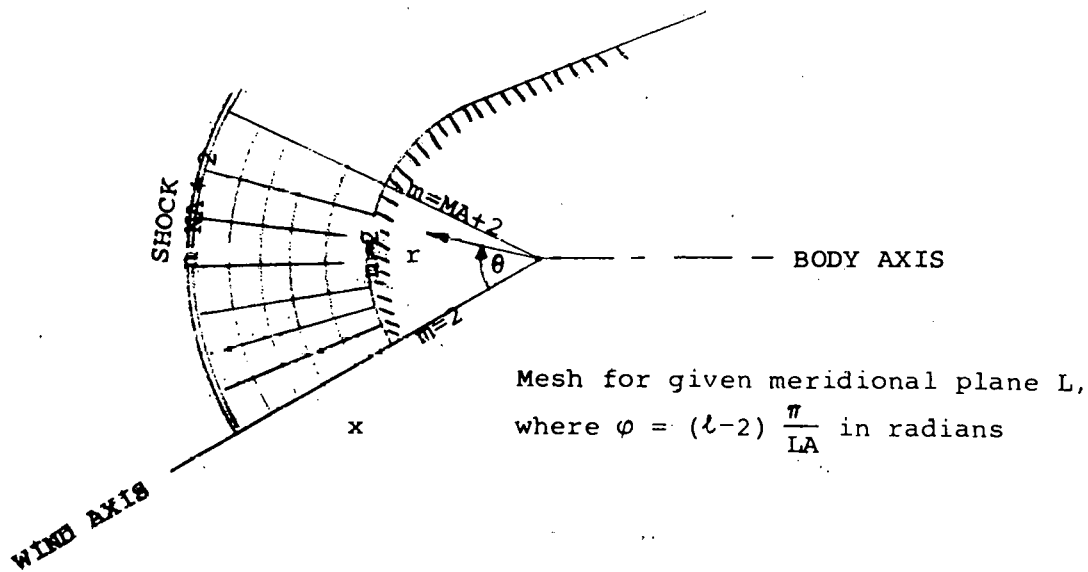
With this sketch the next block of data should be
pretty easy to follow. For the given meridional
plane, whose meridional angle is

$$\varphi = (\ell-2)\ \frac{\pi}{LA}$$

a mesh point is specified by

$$\theta = (m-2)\frac{\theta_{max}}{MA}$$

and

$$r = (n-2)\ \frac{r_{shock}(\theta,\varphi) - r_{body}(\theta,\varphi)}{NA}$$

We also present the values of pressure, (P); density, (RHO); r velocity component, (U); θ velocity component, (V); φ velocity component, (W); entropy (S); Mach number, (M); r, (R); and $(H-H_\infty)/H_\infty$, (DH/HST). All these variables are nondimensionalized as stated in this appendix, part B - 1 - b - i. The far left column, headed by M, is just the running index for θ increasing. The column $(H-H_\infty)/H_\infty$ might look surprising at first since we are considering flows which are inviscid and have constant free stream total enthalpy. However, in making the initial flow field distribution (which is arbitrary) no attempt is made to force the local H to equal H_∞. Thus, the quantity

$(H-H_\infty)/H_\infty$ tells how much of the initial "garbage" has been washed downstream; that is, it is one way of evaluating the steadiness of the flow.

This completes the output of the blunt body solution in the wind-oriented coordinate system. Since people usually prefer body coordinates, the entire flow field is subsequently written out in the body-oriented spherical polar system, R, Θ, Φ, centered at the cone apex. In the body-oriented system, $\Theta = 0$ is on the body axis "downstream," $\Phi = 0$ is in the pitch plane on the leeward side and is positive in the clockwise direction. Note that in the body-oriented system the mesh points do not group into $\Phi =$ constant planes. For a given $\varphi =$ constant, as θ and r vary the corresponding coordinates (R, Θ, Φ) in the body-oriented system all vary (i.e., Φ does not, in general, remain constant). The velocity components, (U, V, W), refer, of course, to the (R, Θ, Φ) directions. With these comments there should be no difficulty interpreting the data for the body-oriented system.

Now, as the blunt body solution proceeds in
time, you will ordinarily output only the initial
(this is always done and you have no choice in the
matter) and final values of the solution, with per-
haps output at a few intermediate stations. For
example, on a 400 time step run you may want to out-
put every 100 steps, or even only the 400th step.
Since each output takes many pages (about 35 for a
5 x 10 x 8 mesh) you may want to keep this output
to a minimum. However, a provision is included so
that you can have the following information at every
step:

 time

 minimum shock standoff distance in pitch plane

 maximum shock velocity $(W_{max}) = (\partial r_{shock}/\partial t)_{max}$

 minimum shock velocity (W_{min})

 maximum range of the shock velocities $\left| W_{max} - W_{min} \right|$

 maximum static pressure

All the above data are, of course, non-dimensional. If
you want this _partial_ _output_ at every step, set LB = 1;
if not, set LB = 0.

So now we have gone through the entire blunt body output. Next the program enters the routine which finds an initial data surface for the conical afterbody solution and obtains the required data on that surface. If everything proceeds as desired, you will next read the data on that initial data surface. Now the data are referred to the R, Θ, Φ system.

The output for the cone program is patterned similarly to that of the blunt body. The data is output on constant R surfaces.

At the top of the page is the step number (remember, this program marches in R, the zero step corresponds to the initial data surface generated from the blunt body solution); the step size ΔR, (DR); the integers indicating the mesh point which is controlling ΔR, (N,M); and the value of R (RADIUS). Remember that R is non-dimensional.

Then there are three pieces of information, two of which are particularly interesting. EXTERNAL MASS FLOW is the free stream mass flow impinging on the shock and is obtained by projecting the free stream velocity on the cross section of the shock wave.

INTERNAL MASS FLOW is the mass flow crossing the R = constant surface between the body and the shock, and is obtained by trapezoidal integration of the flow field solution. These mass flows are nondimensional and, in addition, divided by R^3. Their difference is a measure of the error in the solution and in the integrations. Though it is not possible to really separate the two errors, these data are presented because they are interesting, in spite of the uncertainty in the error. The third datum in this group is the range of the radial deviative of the shock shape; it is:

$$\text{RANGE OF DS/DR} = \left| \left(\frac{\partial \Theta_{shock}}{\partial R} \right)_{max} - \left(\frac{\partial \Theta_{shock}}{\partial R} \right)_{min} \right|$$

This is a measure of the conicity of the flow. Obviously, this number ought to tend to zero as the conical solution is approached (it does!).

Following is a block of data which gives information about the shock. The column of integers is the running index for Φ. Then there is a column of Θ_{shock}, (SHOCK SHAPE), in radii,

$\partial\Theta_{shock}/\partial\Phi$, (DS/DPHI); and $\partial\Theta_{shock}/\partial R$, (DS/DR).

The final blocks of data give the solution of the flow field in the shock layer at each mesh point on the R = constant surface. For clarity, observe the following sketch of the mesh on the constant R surface projected on a plane.

$\Phi = 0$

m=2

Φ, m increasing

Θ, n increasing

n =2

n=NACO + 2

$\Phi = \pi$

m=MACO + 2
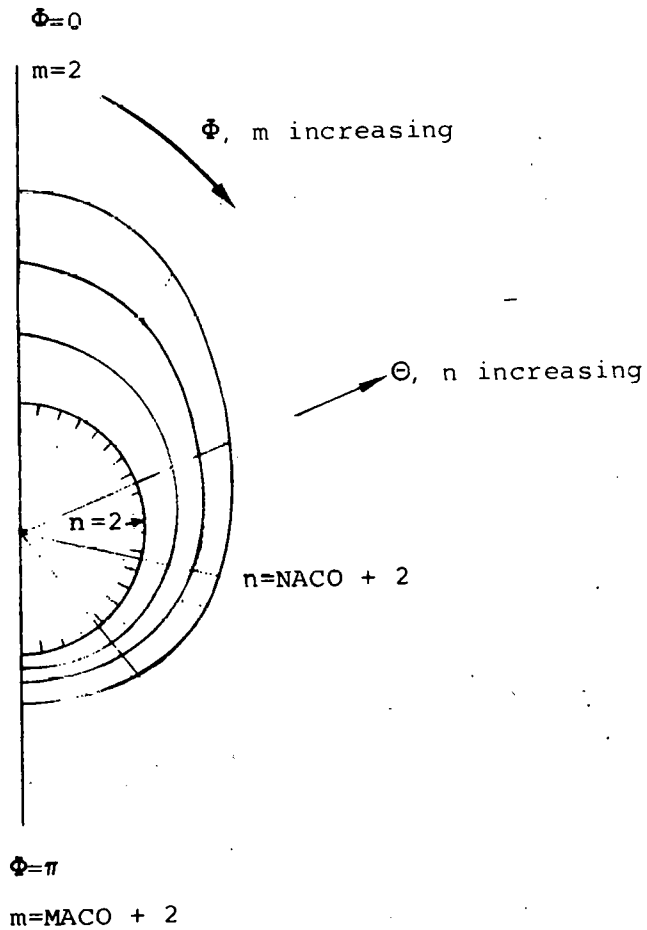
The data is given in blocks corresponding to
n = constant, beginning at the cone surface. There
is a statement indicating the value of n (LINE = N).
For each value of n the data is given at each mesh
point beginning on the leeward pitch plane. First
there is a column, M, which is the running index for
Φ. Then, for that mesh point we have, reading across
the page; pressure, (P); density, (RHO); R velocity
component, (U); Θ velocity component, (V); Φ velocity
component, (W); entropy (S); Mach number, (M); Θ
(THETA). Again, these variables are all nondimensional.
THETA is in radians.

And that ends this discussion of the data output.
There should be little difficulty interpreting the
data.

On the following pages are some of the output for
the case used as the example for the input.

AXISYMMETRIC BLUNT BODY AT ANGLE OF ATTACK WITH CONICAL AFTERBODY, INVISCID
PROGRAM 2J3A

1.5 TO 1 ELLIPSE- 20 DEG. CONE, X0=.5,ALPHA=15   S DECK

RUN NUMBER   1 ON 6/18/68
MA= 5   MA=10   LA= 8   KA= 300   JA=300   LB= 0   LE= 1

FREE STREAM MACH NUMBER= 5.0000000E+00   GAMMA= 1.4000000E+00   STAB= 1.0000000E+00
ALPHA= 1.5000000E+01 DEGREES, THEMAX= 9.0000000E+01 DEGREES

EPS 1 TO 7
  1.000000E-04   1.000000E-04   1.000000E-04   -0.   2.000000E-02   1.000000E-01   -0.

DATA FOR THE CONE ARE
NACO= 10   MACO= 10   KACO= 20   JACO=   2   STABCO= 1.000E+00   RTMAX= 1.6000E+01

THE BODY IS AN ELLIPSOID, AXIS RATIO= 1.500E+00, FOLLOWED BY A 2.000E+01 DEGREE CONE,   X0= 5.0000000E-01

SAMPLE OUTPUT

RODY GEOMETRY DATA

L= 2   PHI(DEG)= 0.

M	THETA(DEG)	R	DR/DTHETA	D2R/DTHETA2	DR/DPHI	D2R/DPHI2	D2R/DTHETA/DPHI
2	0.	1.17513E+00	6.125A7E-02	1.81919E-01	-0.	-0.	-0.
3	9.00000E+00	1.16H0AF+00	2.47432E-02	2.47556E-01	-0.	1.03587E-02	-0.
4	1.80000E+01	1.16702E+00	-1.35243E-02	2.56362E-01	-0.	2.06677E-02	-0.
5	2.70000E+01	1.1721AE+00	-5.09707E-02	2.10592E-01	-0.	2.88061E-02	-0.
6	3.60000E+01	1.18239E+00	-7.40243E-02	9.62395E-02	-0.	3.22729E-02	-0.
7	4.50000E+01	1.19471E+00	-7.50055E-02	-1.29183E-01	-0.	2.74539E-02	-0.
8	5.40000E+01	1.2035IF+00	-2.70930E-02	-5.13672F-01	-0.	8.98451E-03	-0.
9	6.30000E+01	1.19921F+00	9.72578E-02	-1.1A383F+00	-0.	-3.01806E-02	-0.
10	7.20000E+01	1.16790E+00	2.49A32E-01	1.29240E+00	-0.	-7.91375E-02	-0.
11	8.10000E+01	1.14075E+00	7.97A90E-02	1.15191E+00	-0.	-2.23213E-02	-0.
12	9.00000E+01	1.14232E+00	-9.99398E-02	1.159A8E+00	-0.	2.67788E-02	-0.

L= 3   PHI(DEG)= 2.2500E+01

M	THETA(DEG)	R	DR/DTHETA	D2R/DTHETA2	DR/DPHI	D2R/DPHI2	D2R/DTHETA/DPHI
2	0.	1.17513F+00	5.A5957E-02	1.87990E-01	-0.	-0.	-2.34427E-02
3	9.00000F+00	1.16HA6E+00	2.159A3E-02	2.47094F-01	3.93382E-03	9.34372E-03	-2.56791E-02
4	1.80000E+01	1.16H5AF+00	-1.A0947F-02	2.494A2F-01	7.79226E-03	1.82166E-02	-2.25990E-02
5	2.70000E+01	1.17435F+00	-5.3AAA1E-02	1.95997F-01	1.07468E-02	2.45274E-02	-1.39835E-02
6	3.60000E+01	1.18479E+00	-7.58225E-02	6.836A7E-02	1.17930E-02	2.56065E-02	2.18466E-03
7	4.50000E+01	1.19A70F+00	-6.94937E-02	-1.71967F-01	9.47025E-03	1.75299E-02	2.96662E-02
8	5.40000E+01	1.20A02E+00	-1.30540F-02	-5.7A970F-01	1.63210E-03	-5.35240E-03	7.31394E-02
9	6.30000E+01	1.19A62E+00	1.23191E-01	-1.1AA42E+00	-1.44553E-02	-4.97917E-02	1.34292E-01
10	7.20000E+01	1.14224F+00	2.39659F-01	1.24329F+00	-2.67241E-02	-4.72032E-02	-1.46592E-01
11	8.10000E+01	1.13932F+00	5.51065E-02	1.13123F+00	-5.88120E-03	-1.04851E-03	-1.22283E-01
12	9.00000E+01	1.14459F+00	-1.23001E-01	1.15943F+00	1.26125E-02	4.23198E-02	-1.15766E-01

L= 4   PHI(DEG)= 4.5000E+01

M	THETA(DEG)	R	DR/DTHETA	D2R/DTHETA2	DR/DPHI	D2R/DPHI2	D2R/DTHETA/DPHI
2	0.	1.17513F+00	4.33164E-02	2.04A20F-01	-0.	-0.	-4.33164E-02
3	9.00000E+00	1.17107F+00	7.359A2E-03	2.43292F-01	7.10520E-03	6.56179E-03	-4.54234F-02
4	1.80000E+01	1.17290F+00	-3.A25A2E-02	2.2A535F-01	1.37514E-02	1.15638E-02	-3.75092E-02
5	2.70000E+01	1.1A020F+00	-6.A6515F-02	1.4AA53F-01	1.A2946F-02	1.29316E-02	-1.81255E-02
6	3.60000E+01	1.1A1A0F+00	-7.25A73F-02	-1.45321F-02	1.A5997E-02	7.54672E-03	1.75232E-02
7	4.50000E+01	1.2A117F+00	-4.A3294F-02	-3.07339F-01	1.15312E-02	-9.21A42E-03	7.72338E-02
8	5.40000E+01	1.2A339F+00	3.A4713E-02	-7.8AA94F-01	-7.35410E-03	-4.32961E-02	1.68929E-01
9	6.30000E+01	1.1A5A6F+00	2.A5A32E-01	-1.43577F+00	-4.31239E-02	-9.92723E-02	2.89710E-01
10	7.20000E+01	1.14A72F+00	1.A2A5AE-A1	1.14200F+00	-3.27187E-02	1.74531E-02	-2.37870E-01
11	8.10000E+01	1.15A04F+00	-1.20437E-02	1.A9562E+00	2.35249E-03	4.39899E-02	-2.13537E-01
12	9.00000E+01	1.1A364F+00	-1.AA75AF-A1	1.17AA7F+00	3.57637E-02	7.67205E-02	-2.16166E-01

L= 5   PHI(DEG)= 6.7500E+01

AT STEP   0   DT=   0.   AT N=   0, M=   0, L=   0
                                   TIME=   0.

THE FOLLOWING IS IN THE WIND ORIENTED SYSTEM

                    MERIDIONAL PLANE NUMBER   2   PHI(DEG)=   0.
                         THETA   SHOCK VELOCITY   STH   SPH
                    2   0.   0.   0.   0.
                    3   9.00000E+00   0.   -4.51406E-03   0.
                    4   1.80000E+01   0.   -2.22513E-02   0.
                    5   2.70000E+01   0.   -6.16801E-02   0.
                    6   3.60000E+01   0.   -1.26096E-01   0.
                    7   4.50000E+01   0.   -2.16644E-01   0.
                    8   5.40000E+01   0.   -3.35696E-01   0.
                    9   6.30000E+01   0.   -4.89340E-01   0.
                   10   7.20000E+01   0.   -6.89588E-01   0.
                   11   8.10000E+01   0.   -9.57599E-01   0.
                   12   9.00000E+01   0.   -1.32979E+00   0.

AT LINE   2

	P	RHO	U	V	W	S	M	R	DH/HST
2	8.28655E+01	6.00474E+00	0.	-0.	0.	1.90765E+00	0.	1.17513E+00	-9.94760E-14
3	8.16925E+01	5.94391E+00	-1.43433E-02	-6.26480E-01	0.	1.90765E+00	1.42857E-01	1.16808E+00	2.27374E-13
4	7.82992E+01	5.76649E+00	1.44353E-02	-1.24563E+00	0.	1.90765E+00	2.85714E-01	1.16702E+00	8.52651E-14
5	7.30360E+01	5.48654E+00	8.03728E-02	-1.84834E+00	0.	1.90765E+00	4.28571E-01	1.17218E+00	-4.97380E-14
6	6.64060E+01	5.12635E+00	1.56143E-01	-2.42847E+00	0.	1.90765E+00	5.71429E-01	1.18239E+00	-8.52651E-14
7	5.89769E+01	4.70974E+00	1.87393E-01	-2.98485E+00	0.	1.90765E+00	7.14286E-01	1.19471E+00	-9.94760E-14
8	5.12841E+01	4.26230E+00	7.49113E-02	-3.51704E+00	0.	1.90765E+00	8.57143E-01	1.20351E+00	-1.20792E-13
9	4.37763E+01	3.80664E+00	-3.24354E-01	-3.99935E+00	0.	1.90765E+00	1.00000E+00	1.19921E+00	-1.20792E-13
10	4.01985E+01	3.58172E+00	-9.55376E-01	-4.13819E+00	0.	1.90765E+00	1.07143E+00	1.16790E+00	-1.13687E-13
11	3.67790E+01	3.36135E+00	-3.12621E-01	-4.46211E+00	0.	1.90765E+00	1.14286E+00	1.14075E+00	-1.20792E-13
12	3.35380E+01	3.14766E+00	4.08792E-01	-4.67252E+00	0.	1.90765E+00	1.21429E+00	1.14232E+00	-1.20792E-13

AT LINE   3

	P	RHO	U	V	W	S	M	R	DH/HST
2	8.11204E+01	5.91415E+00	-3.40175E-01	0.	0.	1.90765E+00	7.76281E-02	1.20335E+00	4.86673E-03
3	7.98203E+01	5.86612E+00	-3.47230E-01	-7.92077E-01	0.	1.90338E+00	1.98116E-01	1.19776E+00	5.90678E-03
4	7.61424E+01	5.71749E+00	-3.06512E-01	-1.55650E+00	0.	1.89156E+00	3.67410E-01	1.19729E+00	8.98460E-03
5	7.06413E+01	5.48629E+00	-2.13624E-01	-2.27254E+00	0.	1.87445E+00	5.37611E-01	1.20267E+00	1.30247E-02
6	6.39403E+01	5.14521E+00	-6.35317E-02	-2.93094E+00	0.	1.85444E+00	7.05471E-01	1.21372E+00	1.68687E-02
7	5.67661E+01	4.83325E+00	6.19546E-02	-3.53130E+00	0.	1.83321E+00	8.70916E-01	1.22889E+00	1.98127E-02
8	4.96818E+01	4.44967E+00	8.40777E-02	-4.07503E+00	0.	1.81171E+00	1.03298E+00	1.24453E+00	2.21653E-02
9	4.26782E+01	4.05141E+00	-6.62554E-02	-4.54317E+00	0.	1.79030E+00	1.18602E+00	1.25394E+00	2.64860E-02
10	3.86391E+01	3.84417E+00	-6.21247E-02	-4.70204E+00	0.	1.76901E+00	1.25851E+00	1.24727E+00	4.09682E-02
11	3.56134E+01	3.63813E+00	2.74454E-01	-4.57560E+00	0.	1.74766E+00	1.35758E+00	1.25121E+00	4.55558E-02
12	3.15475E+01	3.43312E+00	1.03731E+00	-5.12634E+00	0.	1.72594E+00	1.45720E+00	1.28805E+00	5.00171E-02

AT LINE   4

AT STEP   300   DT=   3.055309BE-03   AT N= 7, M= 5, L= 10
                                      TIME=   8.6744905E-01

THE FOLLOWING IS IN THE WIND ORIENTED SYSTEM

                    MERIDIONAL PLANE NUMBER 2   PHI(DEG)= 0.
                         THETA   SHOCK VELOCITY   STH   SPH
                  2   0.   3.63047E-03   2.45429E-02   0.
                  3   9.00000E+00   3.92035E-03   -3.18246E-02   0.
                  4   1.80000E+01   3.91761E-03   -8.88285E-02   0.
                  5   2.70000E+01   2.61927E-03   -1.42345E-01   0.
                  6   3.60000E+01   7.26052E-03   -2.30528E-01   0.
                  7   4.50000E+01   -6.32625E-03   -2.98998E-01   0.
                  8   5.40000E+01   7.86779E-03   -3.75575E-01   0.
                  9   6.30000E+01   1.59846E-02   -5.34664E-01   0.
                 10   7.20000E+01   -6.94714E-03   -6.73203E-01   0.
                 11   8.10000E+01   -7.59558E-03   -8.85995E-01   0.
                 12   9.00000E+01   -8.24401E-03   -1.20271E+00   0.

AT LINE   2
        P   RHO   U   V   W   S   M   R   DH/HST
  2 8.31961E+01   6.02165E+00 -6.10812E-03 -1.17172E-01   0.   1.90765E+00   2.66786E-02   1.17513E+00 -1.28085E-03
  3 8.04664E+01   5.88005E+00 -2.10524E-02 -9.19519E-01   1.08510E-20   1.90765E+00   2.10133E-01   1.16808E+00 -3.98692E-04
  4 7.47722E+01   5.57973E+00   1.96870E-02 -1.69881E+00 -2.98536E-20   1.90765E+00   3.92235E-01   1.16702E+00 -9.42658E-04
  5 6.60901E+01   5.10888E+00   1.06320E-01 -2.44505E+00   4.13814E-20   1.90765E+00   5.75080E-01   1.17218E+00   5.80263E-04
  6 5.58956E+01   4.53268E+00   2.06910E-01 -3.21808E+00 -4.71841E-20   1.90765E+00   7.76089E-01   1.18239E+00 -1.24783E-03
  7 4.15562E+01   3.66772E+00   2.66104E-01 -4.23859E+00   6.86009E-20   1.90765E+00   1.06633E+00   1.19471E+00 -7.74581E-03
  8 2.73429E+01   2.71945E+00   1.15675E-01 -5.15558E+00 -6.32077E-20   1.90765E+00   1.37459E+00   1.20351E+00 -3.77774E-03
  9 1.30238E+01   1.60128E+00 -5.28471E-01 -6.51615E+00   9.47456E-20   1.90765E+00   1.93739E+00   1.19921E+00 -3.18102E-02
 10 4.69460E+00   7.72576E-01 -1.66375E+00 -7.20668E+00 -8.54787E-20   1.90765E+00   2.53575E+00   1.16790E+00 -6.59705E-03
 11 4.66940E+00   7.69621E-01 -5.16085E-01 -7.38035E+00 -8.92500E-20   1.90765E+00   2.53850E+00   1.14075E+00 -6.28065E-03
 12 4.66450E+00   7.66677E-01   6.45015E-01 -7.37255E+00 -9.30212E-20   1.90765E+00   2.54124E+00   1.14232E+00 -5.96539E-03

AT LINE   3
        P   RHO   U   V   W   S   M   R   DH/HST
  2 8.29330E+01   6.05664E+00 -3.31139E-01   1.00157E-02   0.   1.89642E+00   7.56651E-02   1.21119E+00   6.61550E-03
  3 8.07443E+01   5.94794E+00 -3.11869E-01 -9.12847E-01   4.45360E-16   1.89502E+00   2.21276E-01   1.20579E+00   6.65892E-03
  4 7.51935E+01   5.68005E+00 -2.79557E-01 -1.79983E+00   4.98149E-16   1.88832E+00   4.23088E-01   1.20671E+00   6.36835E-03
  5 6.70380E+01   5.25231E+00 -1.59442E-01 -2.57664E+00   3.92015E-16   1.88312E+00   6.10715E-01   1.21465E+00   6.11533E-03
  6 5.75507E+01   4.75000E+00 -4.01958E-02 -3.39689E+00   3.97970E-16   1.87028E+00   8.25215E-01   1.22795E+00   3.36882E-03
  7 4.45063E+01   4.00675E+00   4.38962E-02 -4.28773E+00   5.41750E-16   1.85246E+00   1.08751E+00   1.24716E+00   4.69618E-03
  8 3.19423E+01   3.14229E+00   1.44149E-01 -5.07318E+00   5.50173E-16   1.84392E+00   1.35345E+00   1.26363E+00   5.54291E-03
  9 1.95463E+01   2.25015E+00   8.87395E-02 -6.02843E+00   4.43805E-16   1.83729E+00   1.72895E+00   1.27435E+00 -5.69701E-03
 10 8.93672E+00   1.27379E+00 -4.79440E-01 -6.86595E+00   5.51519E-16   1.85137E+00   2.20247E+00   1.26874E+00 -1.62509E-03
 11 6.68363E+00   1.03840E+00   1.75098E-03 -7.15316E+00   5.39319E-16   1.84691E+00   2.38364E+00   1.26989E+00   3.58495E-03
 12 6.99858E+00   6.46516E-01   6.29635E-01 -7.42038E+00   5.27119E-16   1.84245E+00   2.59688E+00   1.30394E+00 -5.02025E-03

AT LINE   4

THE FOLLOWING IS IN BODY ORIE TED COORDINATES

TRANSFORMED MERIDIONAL PLANE NUMBER 2

AT LINE   2

M	THETA	PHI	P	RHO	U	V	W	S	M	R
2	-7.4991E+00	0.	8.3196E+01	6.0218E+00	-3.9966E-02	1.1031E-01	0.	1.9076E+00	2.6679E-02	2.2131E+00
3	-3.2271E+00	0.	8.0466E+01	5.8801E+00	-1.2666E-01	9.1100E-01	1.0851E-20	1.9076E+00	2.1013E-01	2.1690E+00
4	1.4184E+00	0.	7.4772E+01	5.5797E+00	1.1716E-01	1.6949E+00	-2.9854E-20	1.9076E+00	3.9224E-01	2.1626E+00
5	6.3770E+00	0.	6.6390E+01	5.1089E+00	6.6995E-01	2.3539E+00	4.1381E-20	1.9076E+00	5.7508E-01	2.1942E+00
6	1.0790E+01	0.	5.5696E+01	4.5327E+00	1.5194E+00	2.8443E+00	-4.7184E-20	1.9076E+00	7.7609E-01	2.2634E+00
7	1.4604E+01	0.	4.1556E+01	3.6677E+00	2.7869E+00	3.2046E+00	6.8601E-20	1.9076E+00	1.0663E+00	2.3691E+00
8	1.7570E+01	0.	2.7343E+01	2.7198E+00	4.2389E+00	2.9368E+00	-6.3208E-20	1.9076E+00	1.3746E+00	2.5089E+00
9	1.9442E+01	0.	1.3224E+01	1.6013E+00	5.2203E+00	2.0117E+00	9.4746E-20	1.9076E+00	1.9374E+00	2.6774E+00
10	2.0000E+01	0.	4.6946E+00	7.7258E-01	7.3960E+00	5.6843E-14	-8.5479E-20	1.9076E+00	2.5357E+00	2.8638E+00
11	2.0000E+01	0.	4.6695E+00	7.6962E-01	7.3984E+00	8.5265E-14	-8.9250E-20	1.9076E+00	2.5385E+00	3.0470E+00
12	2.0000E+01	0.	4.6445E+00	7.6668E-01	7.4007E+00	7.1054E-14	-9.3021E-20	1.9076E+00	2.5412E+00	3.2261E+00

AT LINE   3

M	THETA	PHI	P	RHO	U	V	W	S	M	R
2	-8.2679E+00	0.	8.2634E+01	6.0566E+00	3.0814E-01	1.2161E-01	0.	1.8964E+00	7.5665E-02	2.1799E+00
3	-3.3896E+00	0.	8.0744E+01	5.9479E+00	1.5876E-01	9.5150E-01	4.4536E-16	1.8950E+00	2.2128E-01	2.1318E+00
4	1.7046E+00	0.	7.5193E+01	5.6800E+00	4.2623E-01	1.7708E+00	4.9815E-16	1.8883E+00	4.2309E-01	2.1231E+00
5	6.7331E+00	0.	6.7038E+01	5.2523E+00	9.7869E-01	2.3888E+00	3.9202E-16	1.8831E+00	6.1071E-01	2.1540E+00
6	1.1408E+01	0.	5.7508E+01	4.7508E+00	1.8545E+00	2.8463E+00	3.9797E-16	1.8703E+00	8.2522E-01	2.2248E+00
7	1.5509E+01	0.	4.4506E+01	4.0068E+00	2.9999E+00	3.0647E+00	5.4175E-16	1.8525E+00	1.0875E+00	2.3320E+00
8	1.8731E+01	0.	3.1962E+01	3.1823E+00	4.2127E+00	2.8304E+00	5.5017E-16	1.8439E+00	1.3534E+00	2.4763E+00
9	2.0943E+01	0.	1.5944E+01	2.2501E+00	5.5940E+00	2.2488E+00	4.4380E-16	1.8373E+00	1.7290E+00	2.6495E+00
10	2.1981E+01	0.	8.9347E+00	1.2738E+00	6.8506E+00	8.4559E-01	5.5152E-16	1.8514E+00	2.2025E+00	2.8428E+00
11	2.2424E+01	0.	6.6636E+00	1.0384E+00	7.1457E+00	3.7125E-01	5.3932E-16	1.8469E+00	2.3836E+00	3.0407E+00
12	2.2645E+01	0.	4.9946E+00	8.4651E-01	7.4642E+00	-1.9093E-01	5.2712E-16	1.8424E+00	2.5969E+00	3.2442E+00

AT LINE   4

M	THETA	PHI	P	RHO	U	V	W	S	M	R
2	-8.6482E+00	0.	8.2640E+01	6.0021E+00	5.9346E-01	2.4608E-01	0.	1.8983E+00	1.4683E-01	2.1468E+00
3	-3.5579E+00	0.	7.0742E+01	5.9342E+00	4.2794E-01	1.1026E+00	-8.7485E-17	1.8860E+00	2.7266E-01	2.0946E+00
4	1.7941E+00	0.	7.4743E+01	5.7163E+00	7.1745E-01	1.8942E+00	8.8609E-17	1.8734E+00	4.7341E-01	2.0835E+00
5	7.1028E+00	0.	6.7679E+01	5.3505E+00	1.3034E+00	2.5275E+00	-1.1072E-16	1.8578E+00	6.7880E-01	2.1138E+00
6	1.2048E+01	0.	5.8684E+01	4.9615E+00	2.2027E+00	2.9440E+00	-1.2815E-16	1.8250E+00	9.0572E-01	2.1864E+00
7	1.4443E+01	0.	4.6605E+01	4.3441E+00	3.2737E+00	3.0701E+00	1.2163E-16	1.7854E+00	1.1581E+00	2.2956E+00
8	1.4923E+01	0.	3.5150E+01	3.6160E+00	4.3596E+00	2.8337E+00	3.4531E-17	1.7601E+00	1.4095E+00	2.4448E+00
9	2.2474E+01	0.	2.5013E+01	2.9038E+00	5.3846E+00	2.3474E+00	-1.9286E-17	1.7270E+00	1.6915E+00	2.6235E+00

AT STEP   6   DR= 30.5530979E-04   AT N= 7, M= 5

                                    RADIUS= 31.2549022E-01

EXTERNAL MASS FLOW= 34.033777E-01   INTERNAL MASS FLOW= 34.914715E-01
RANGE OF DS/DR= 93.9342271E-03

                          SHOCK SHAPE   DS/DPHI   DS/DR
                    2   5.67064E-01   0.   1.10081E-01
                    3   5.62381E-01   -2.56416E-02   1.02217E-01
                    4   5.50953E-01   -4.14770E-02   7.95860E-02
                    5   5.36320E-01   -5.21486E-02   6.47531E-02
                    6   5.16187E-01   -5.87043E-02   6.43512E-02
                    7   4.99435E-01   -5.75270E-02   4.49383E-02
                    8   4.82041E-01   -5.16380E-02   4.74693E-02
                    9   4.66990E-01   -4.10101E-02   1.77574E-02
                   10   4.56274E-01   -2.77708E-02   1.96550E-02
                   11   4.49541E-01   -1.41597E-02   2.19730E-02
                   12   4.47377E-01   0.   1.61432E-02

                                        AT LINE   2
         P   RHO   U   V   W   S   M   THETA
 2   4.63228E+00   7.64408E-01   7.37952E+00 -1.13899E-02 -7.54604E-17   1.90916E+00   2.53355E+00   3.49066E-01 -2.86933E-03
 3   4.89555E+00   7.95145E-01   7.30973E+00   1.65460E-02 -5.87979E-01   1.90918E+00   2.49788E+00   3.49066E-01 -2.83236E-03
 4   5.55853E+00   8.70920E-01   7.14197E+00   1.86667E-02 -1.09987E+00   1.90882E+00   2.41743E+00   3.49066E-01 -3.04632E-03
 5   6.73893E+00   9.98805E-01   6.88229E+00   4.96645E-04 -1.47233E+00   1.90958E+00   2.28998E+00   3.49066E-01 -1.68300E-03
 6   8.70304E+00   1.19874E+00   6.57240E+00 -2.27750E-03 -1.67262E+00   1.90989E+00   2.12735E+00   3.49066E-01 -2.28037E-03
 7   1.13579E+01   1.44955E+00   6.21463E+00 -5.90276E-03 -1.77202E+00   1.91016E+00   1.95098E+00   3.49066E-01 -2.49728E-05
 8   1.46805E+01   1.73875E+00   5.87376E+00 -1.14977E-02 -1.64473E+00   1.91208E+00   1.77416E+00   3.49066E-01   3.02253E-03
 9   1.85336E+01   2.05595E+00   5.60754E+00 -1.37730E-02 -1.35932E+00   1.91055E+00   1.62419E+00   3.49066E-01   2.12681E-03
10   2.21948E+01   2.33543E+00   5.35778E+00   3.07477E-03 -9.86871E-01   1.91238E+00   1.49337E+00   3.49066E-01   4.17361E-03
11   2.46862E+01   2.52303E+00   5.27326E+00   3.53419E-03 -5.60987E-01   1.91060E+00   1.43282E+00   3.49066E-01 -1.30249E-04
12   2.56141E+01   2.59256E+00   5.27037E+00   6.09348E-03   2.72316E-13   1.90944E+00   1.41711E+00   3.49066E-01 -3.47543E-03

                                        AT LINE   3
         P   RHO   U   V   W   S   M   THETA
 2   5.17899E+00   8.45628E-01   7.33048E+00   5.26204E-02   1.82393E-16   1.87935E+00   2.50367E+00   3.70866E-01 -1.76035E-04
 3   5.47533E+00   8.80748E-01   7.26154E+00   8.46304E-02 -5.78379E-01   1.87803E+00   2.46938E+00   3.70397E-01   1.19024E-04
 4   6.21521E+00   9.66342E-01   7.09409E+00   9.10400E-02 -1.07893E+00   1.87409E+00   2.39155E+00   3.69255E-01   8.44976E-04
 5   7.42968E+00   1.09970E+00   6.85319E+00   4.91790E-02 -1.44787E+00   1.87232E+00   2.27767E+00   3.67791E-01   2.54667E-03
 6   9.20034E+00   1.28272E+00   6.58466E+00 -3.23060E-02 -1.65758E+00   1.87066E+00   2.14402E+00   3.65978E-01   2.41747E-03
 7   1.17944E+01   1.53614E+00   6.27464E+00 -7.65209E-02 -1.75760E+00   1.86671E+00   1.98754E+00   3.64103E-01   4.00252E-03
 8   1.50596E+01   1.82625E+00   5.94575E+00 -1.09977E-01 -1.63373E+00   1.86885E+00   1.81505E+00   3.62363E-01   8.73090E-03
 9   1.88618E+01   2.14749E+00   5.67995E+00 -1.34760E-01 -1.35799E+00   1.86699E+00   1.66595E+00   3.60858E-01   1.03457E-02
10   2.23935E+01   2.42575E+00   5.45469E+00 -1.41677E-01 -9.93822E-01   1.86856E+00   1.54305E+00   3.59787E-01   1.22148E-02
11   2.48446E+01   2.61452E+00   5.36312E+00 -1.46972E-01 -5.62479E-01   1.86897E+00   1.47769E+00   3.59113E-01   8.93223E-03
12   2.58152E+01   2.66518E+00   5.34428E+00 -1.49133E-01   2.77767E-13   1.86812E+00   1.45728E+00   3.58897E-01   7.44119E-03

                                        AT LINE   4
         P   RHO   U   V   W   S   M   THETA
 2   5.40981E+00   9.37798E-01   7.28437E+00   1.26642E-01   4.40902E-16   1.84946E+00   2.47415E+00   3.92665E-01   1.46685E-03
 3   6.14280E+00   9.77727E-01   7.21663E+00   1.60161E-01 -5.68506E-01   1.84679E+00   2.44139E+00   3.91729E-01   2.02681E-03
 4   6.96710E+00   1.07413E+00   7.04944E+00   1.63540E-01 -1.05760E+00   1.84083E+00   2.36640E+00   3.89443E-01   3.75231E-03
 5   8.20342E+00   1.21225E+00   6.82703E+00   1.01198E-01 -1.42323E+00   1.83508E+00   2.26595E+00   3.86517E-01   6.06882E-03
 6   9.73324E+00   1.37331E+00   6.60407E+00 -6.19157E-02 -1.64247E+00   1.83143E+00   2.16077E+00   3.82890E-01   6.83995E-03

REFERENCES

1. Moretti, G. and Abbett, M., "A Time Dependent Computational Method for Blunt Body Flows," AIAA J. 4, 12, Dec. 1966, pp. 2136-2141.

2. Moretti, G. and Bleich, G., "Three-Dimensional Flow About Blunt Bodies," AIAA J.,5, 9, Sept. 1967, pp. 1557-1562.

3. Moretti, G., "Inviscid Flow Field Past a Pointed Cone at an Angle of Attack," GASL TR-577, December 15, 1965.

4. Moretti, G., "Three-Dimensional Inviscid Flow About Supersonic Blunt Cones at Angle of Attack," Volume II, "Improved Time-Dependent Techniques for the Blunt-Body Problem," SC-CR-68-3728, September 1968.

5. Lax, P. D. and Wendroff, B., "System of Conservation Laws," Commun. Pure Appl. Math, 13, 1960, pp. 217-237.

6. Lax, P. D. and Wendroff, B., "Difference Schemes for Hyperbolic Equation with High Order of Accuracy," Commun. Pure Appl. Math, XVII, 1964, pp. 381-398.

7. Burstein, S. Z., "Numerical Methods in Multidimensional Shocked Flows," AIAA J., 2, 12, Dec. 1964, pp. 2111-2117.

8. Babenko, K. I., "Three-Dimensional Flow of Ideal Gas Past Smooth Bodies," NASA TTF-380, April 1966.

M   Mach Number

V_∞ Free Stream Velocity

M > 1

M < 1

V_∞

M > 1

Blunted Cone

Bow Shock Wave
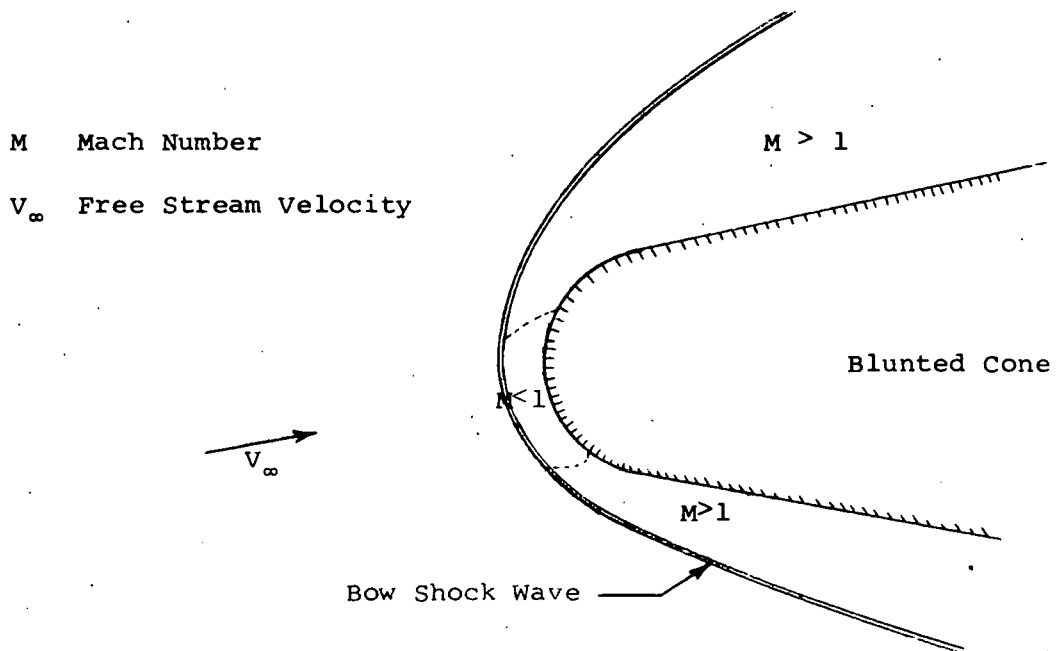
FIGURE 1: SCHEMATIC OF FLOW FIELD (IN PITCH PLANE) ABOUT A BLUNTED CONE

Flow Field Computed
in this Region

Bow Shock

——— Sonic Surface

$M_\infty > 1$
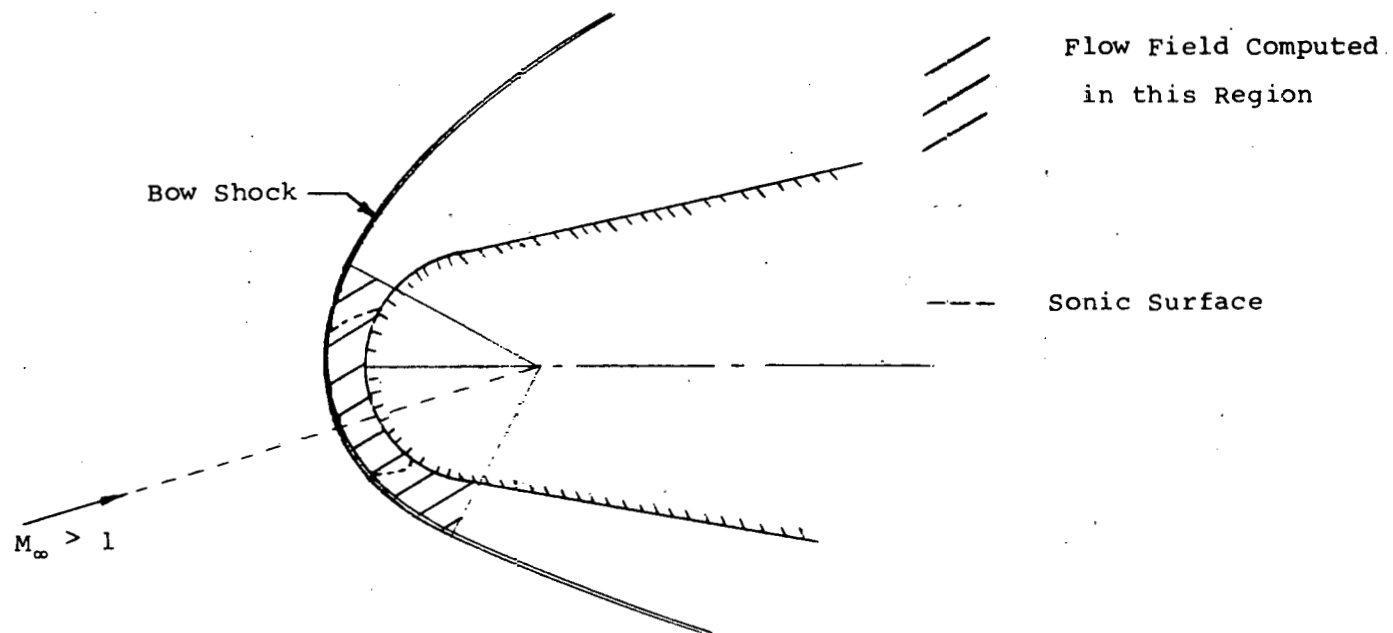
FIGURE 2: SCHEMATIC OF THE REGION COMPUTED BY THE BLUNT BODY
SOLUTION (IN PITCH PLANE)
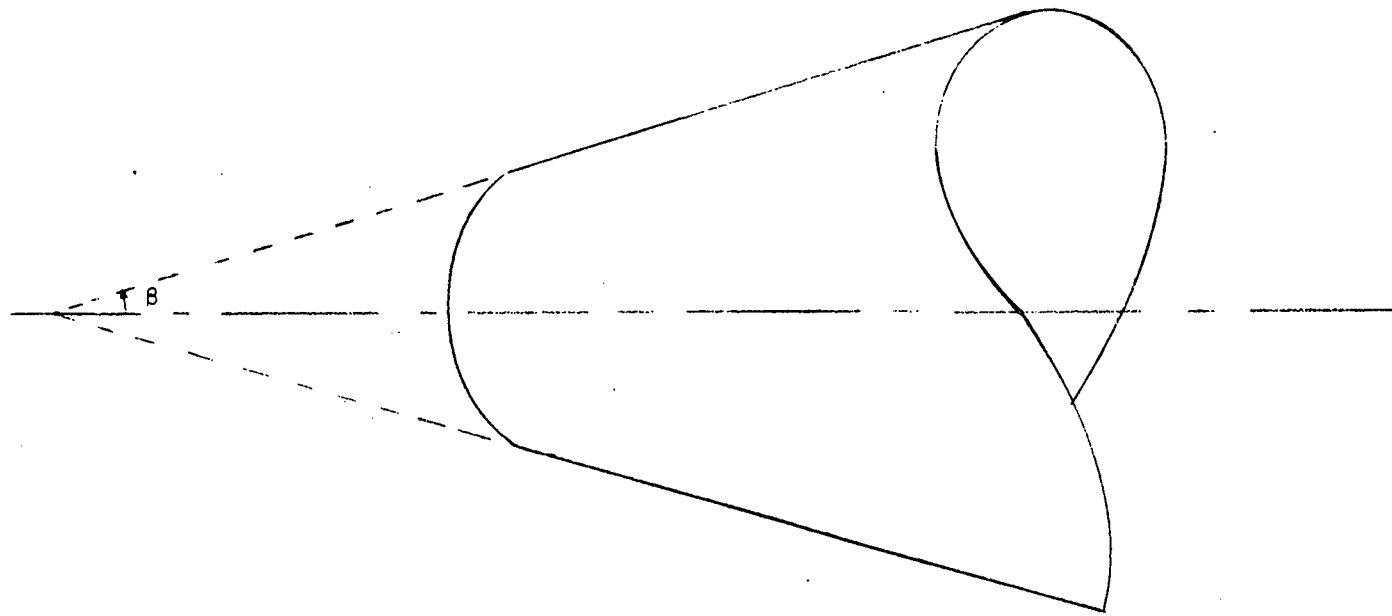
FIGURE 3:   BLUNT BODY FOLLOWED BY A RIGHT CIRCULAR CONE
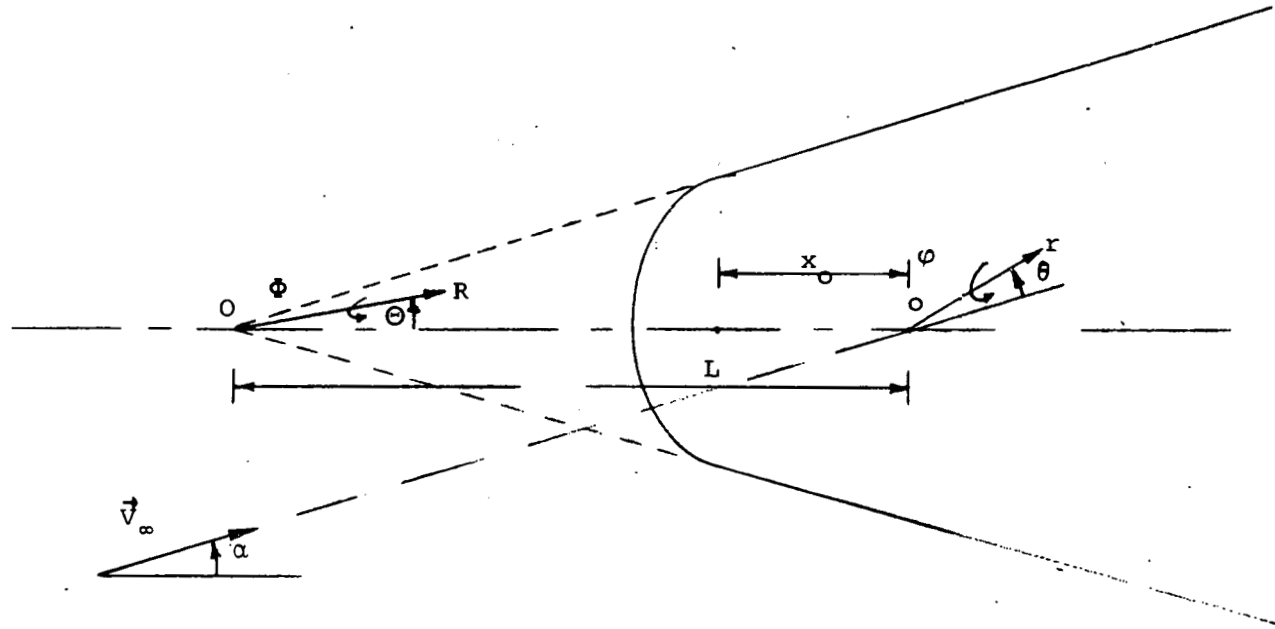
FIGURE 4: COORDINATE SYSTEMS
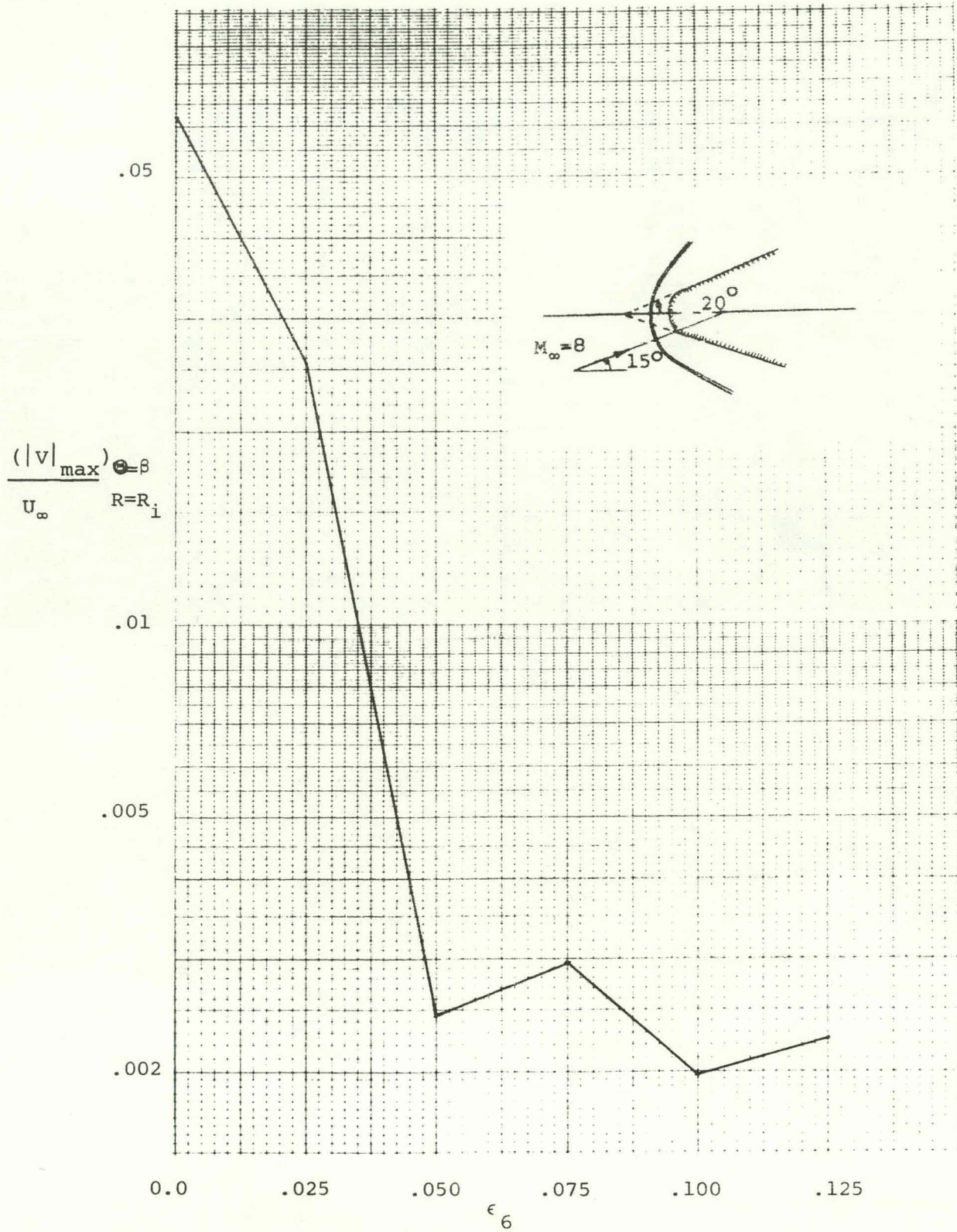
FIGURE 5:   EFFECT OF ϵ_6 ON INTERPOLATION ERRORS AT THE BODY SURFACE
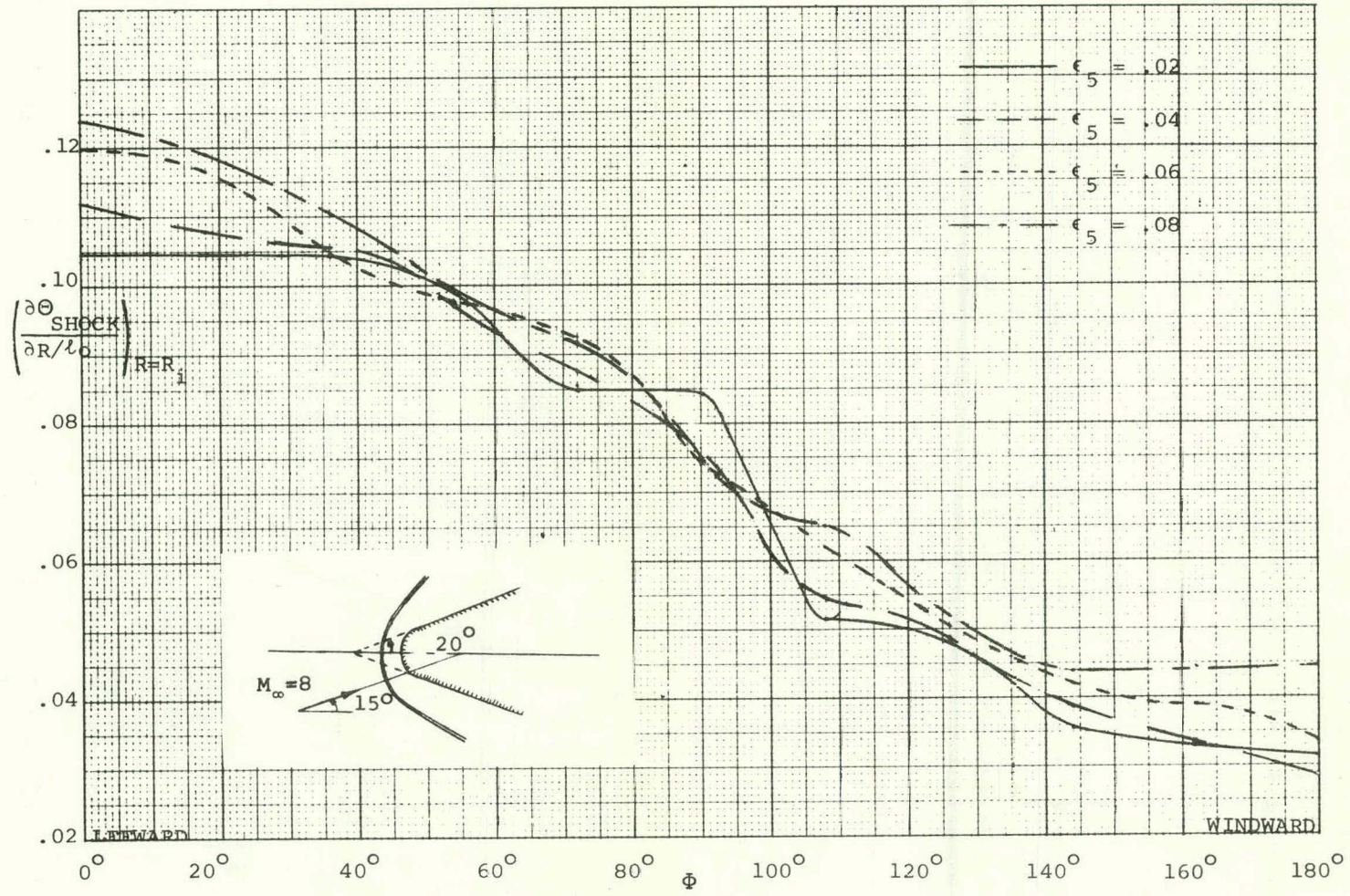
FIGURE 6: DEPENDENCE OF $\left(\partial\Theta_{SHOCK}\middle/\partial(R/\ell_0)\right)_{R=R_i}$ ON THE PARAMETER ϵ_5
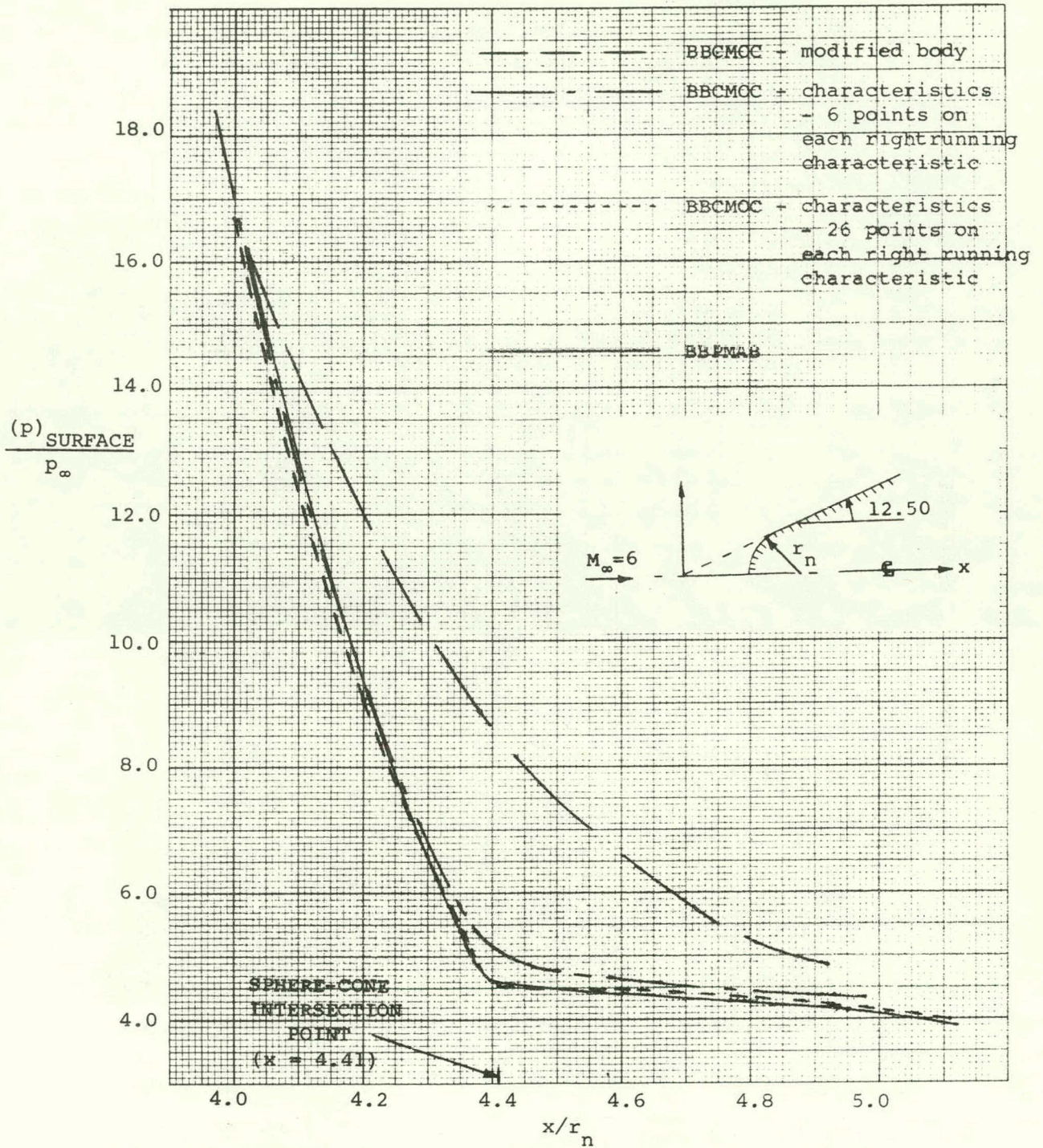
FIGURE 7: PRESSURE COMPARISON IN THE VICINITY OF THE ATTACHMENT POINT –
12½ DEGREE HALF-ANGLE SPHERICALLY TIPPED CONE
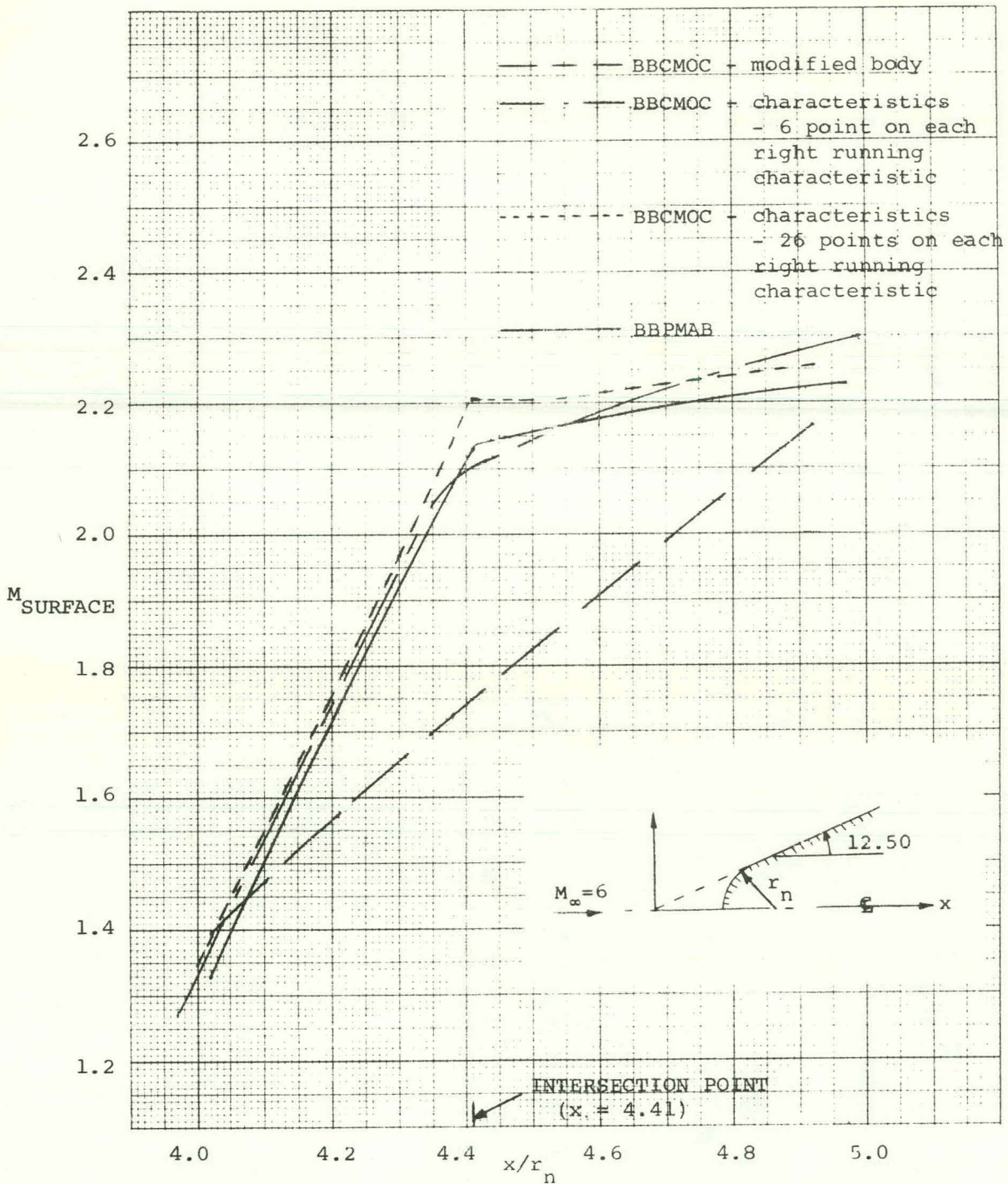
FIGURE 8: SURFACE MACH NUMBER COMPARISON NEAR THE ATTACHMENT POINT –
12½ DEGREE HALF-ANGLE SPHERICALLY TIPPED CONE, ZERO
INCIDENCE
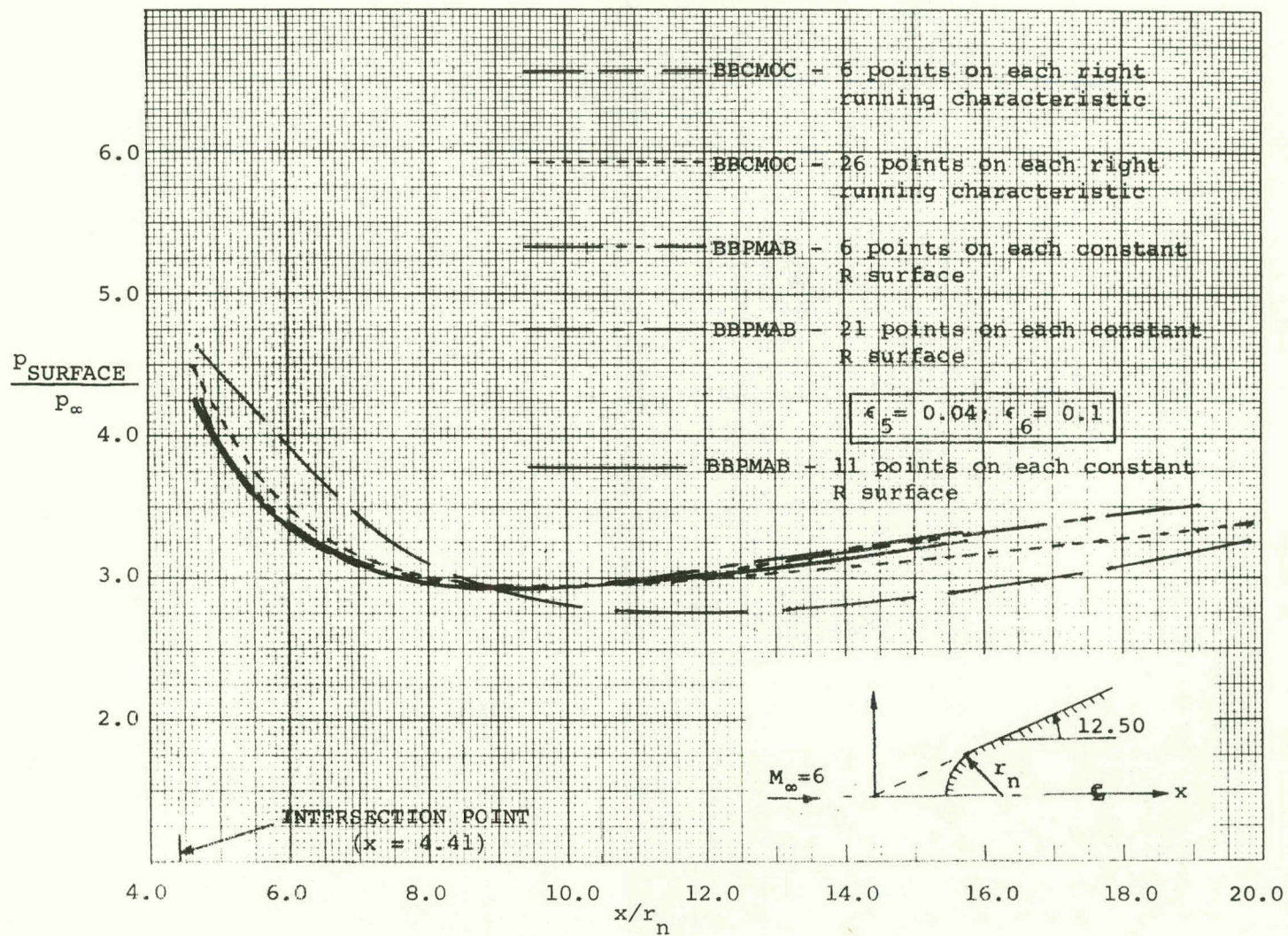
FIGURE 9: SURFACE PRESSURE COMPARISON DOWNSTREAM OF ATTACHMENT POINT - SPHERICALLY
TIPPED 12½ DEGREE HALF-ANGLE CONE, ZERO INCIDENCE
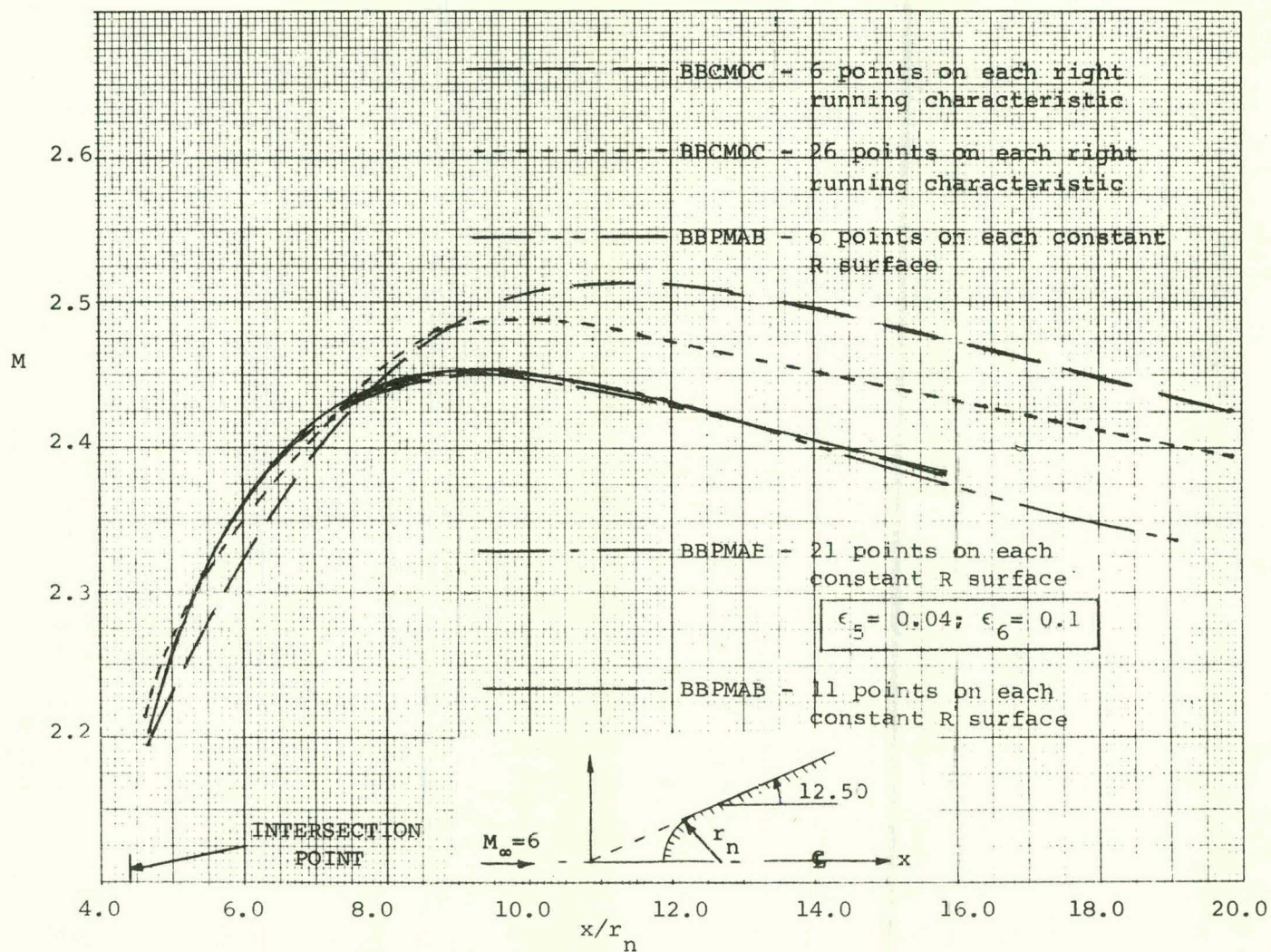
FIGURE 10: SURFACE MACH NUMBER COMPARISON DOWNSTREAM OF ATTACHMENT POINT - SPHERICALLY TIPPED 12½ DEGREE CONE - ZERO INCIDENCE
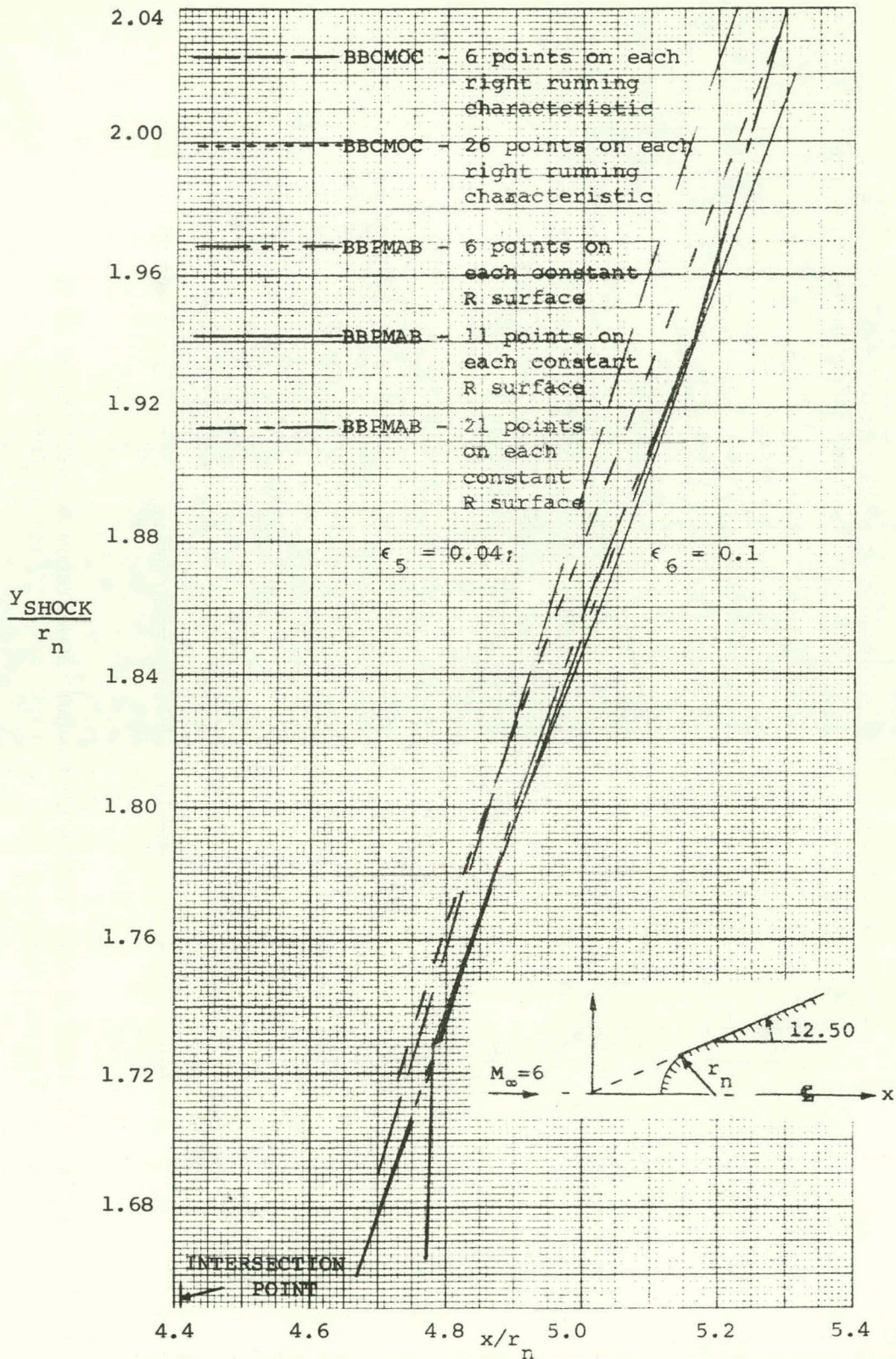
FIGURE 11: SHOCK POSITION NEAR THE INITIAL DATA SURFACE - SPHERICALLY TIPPED 12½ DEGREE HALF-ANGLE CONE - ZERO INCIDENCE
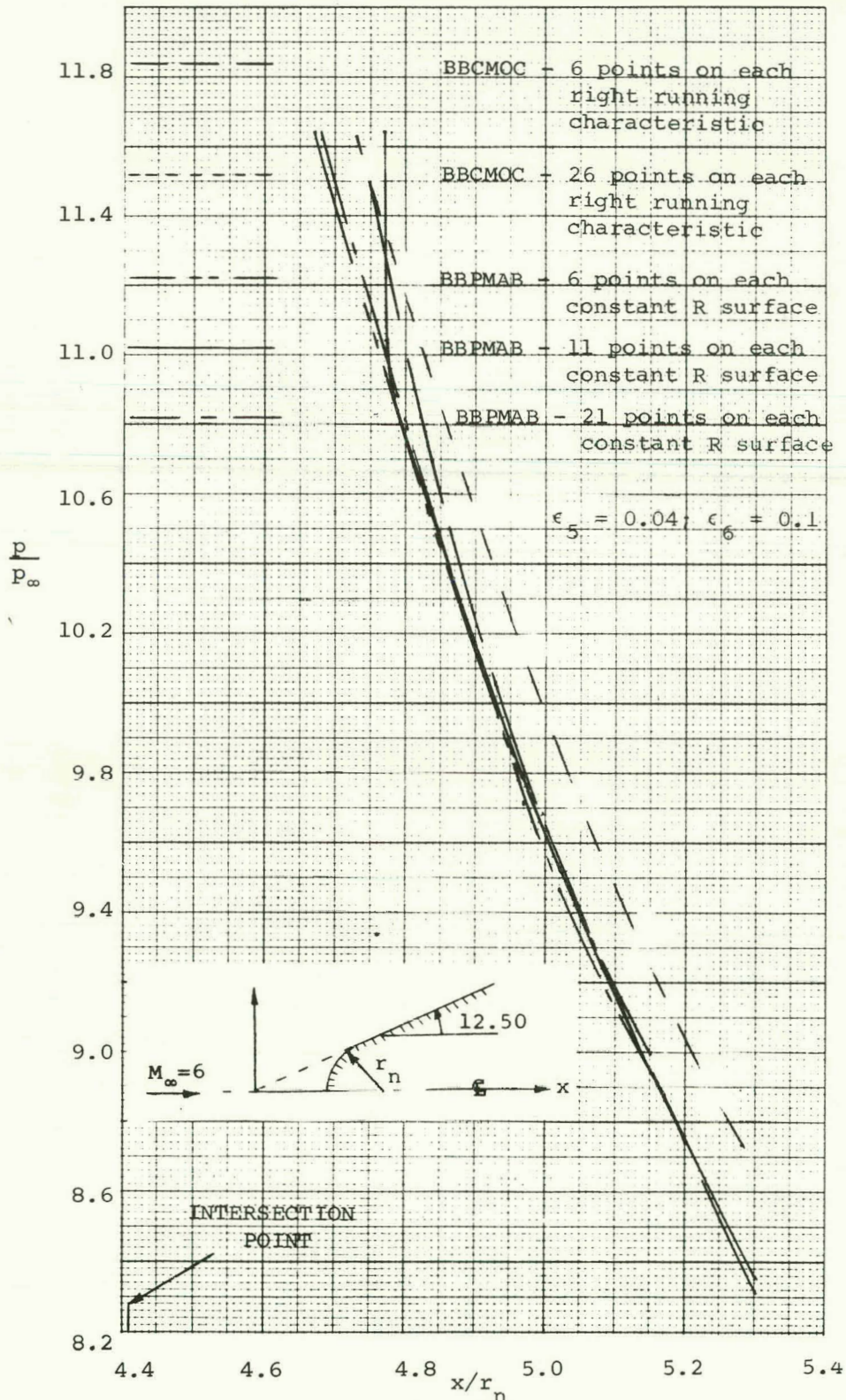
FIGURE 12: PRESSURE BEHIND THE SHOCK NEAR THE INITIAL DATA
SURFACE - SPHERICALLY TIPPED 12½ DEGREE HALF-
ANGLE CONE - ZERO INCIDENCE
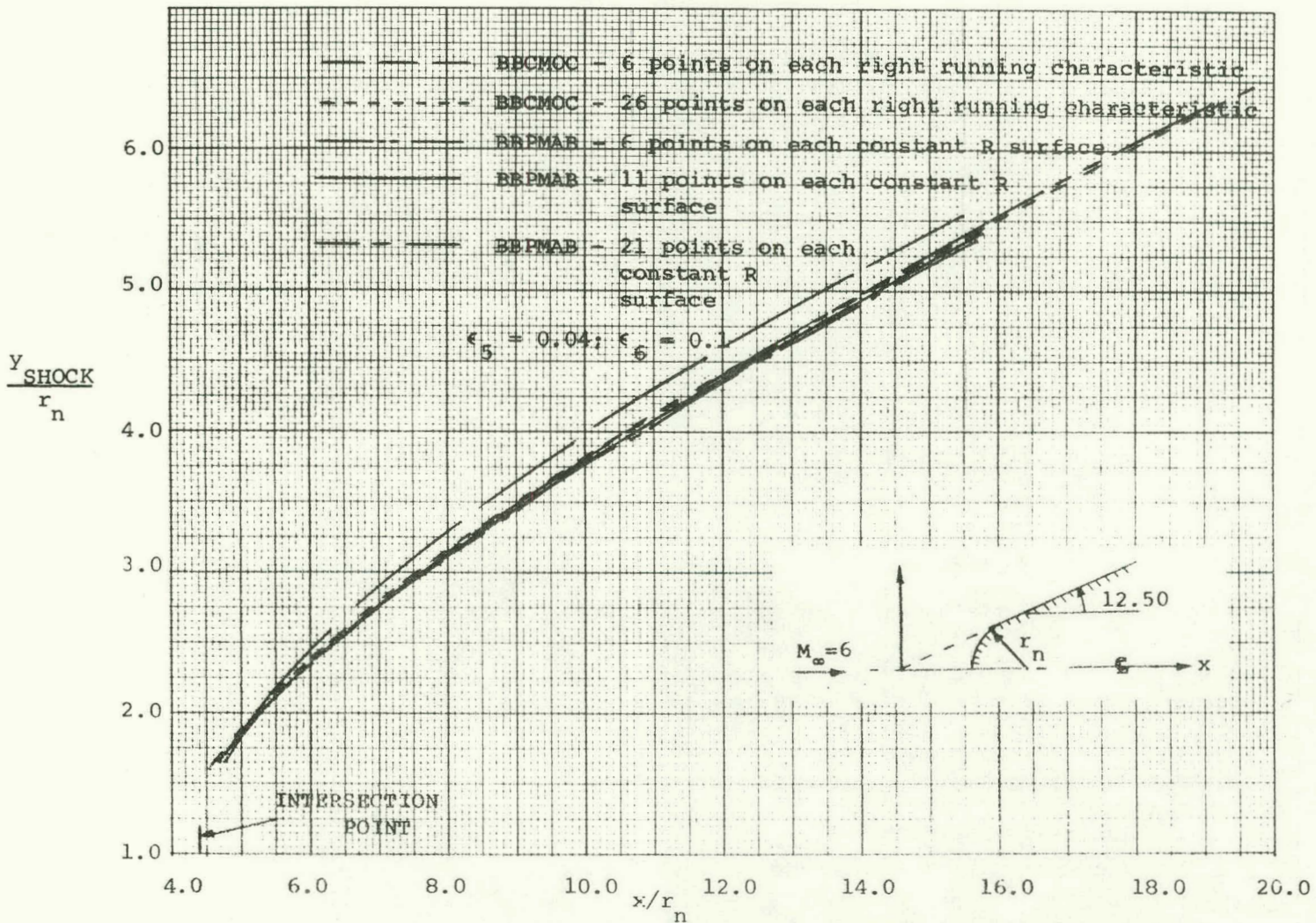
FIGURE 13: SHOCK SHAPE DOWNSTREAM OF INITIAL DATA SURFACE - SPHERICALLY
TIPPED 12½ DEGREE HALF-ANGLE CONE - ZERO INCIDENCE
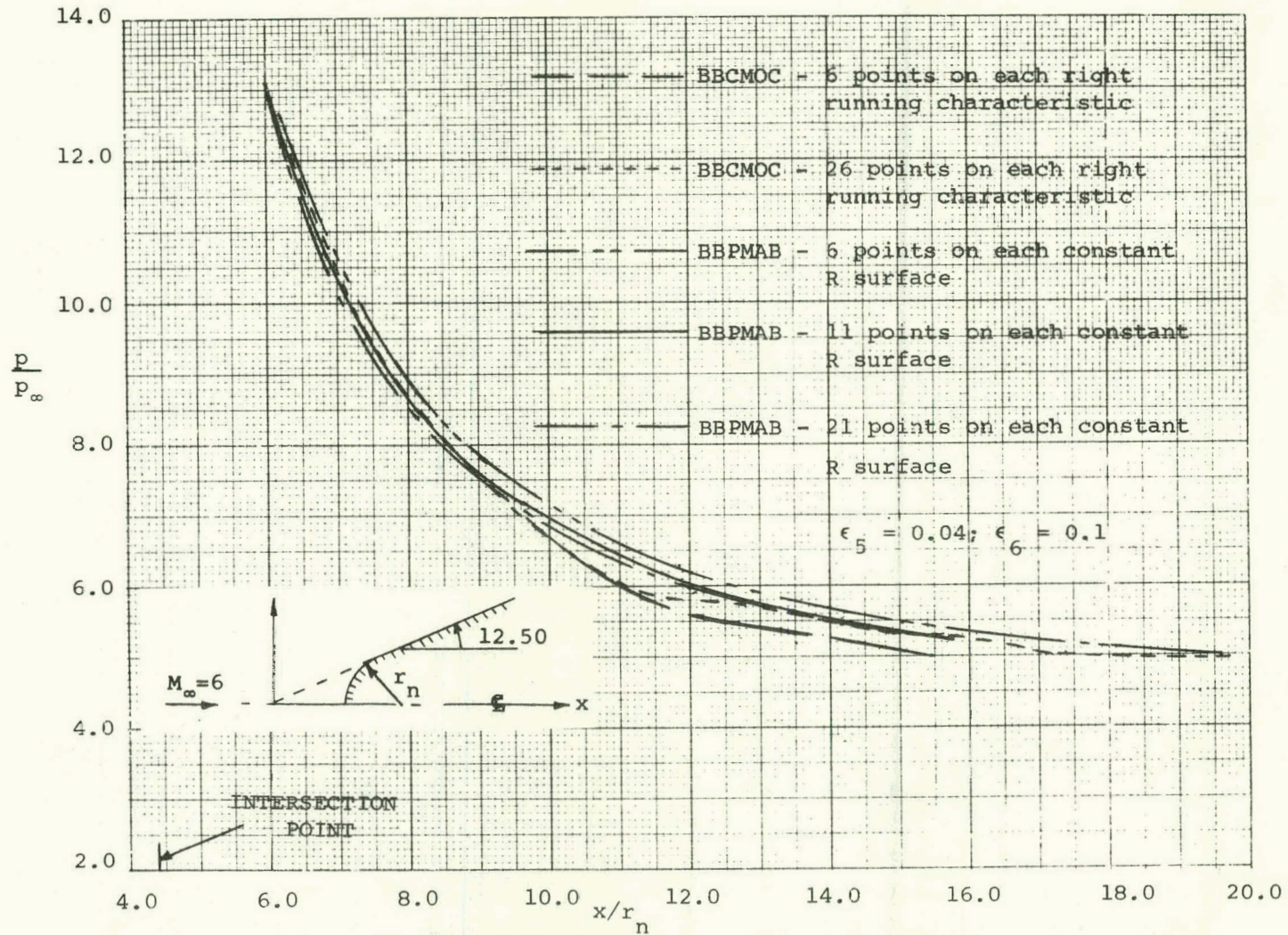
FIGURE 14: PRESSURE BEHIND SHOCK DOWNSTREAM OF INITIAL DATA SURFACE SPHERICALLY TIPPED 12½ DEGREE HALF-ANGLE CONE - ZERO INCIDENCE
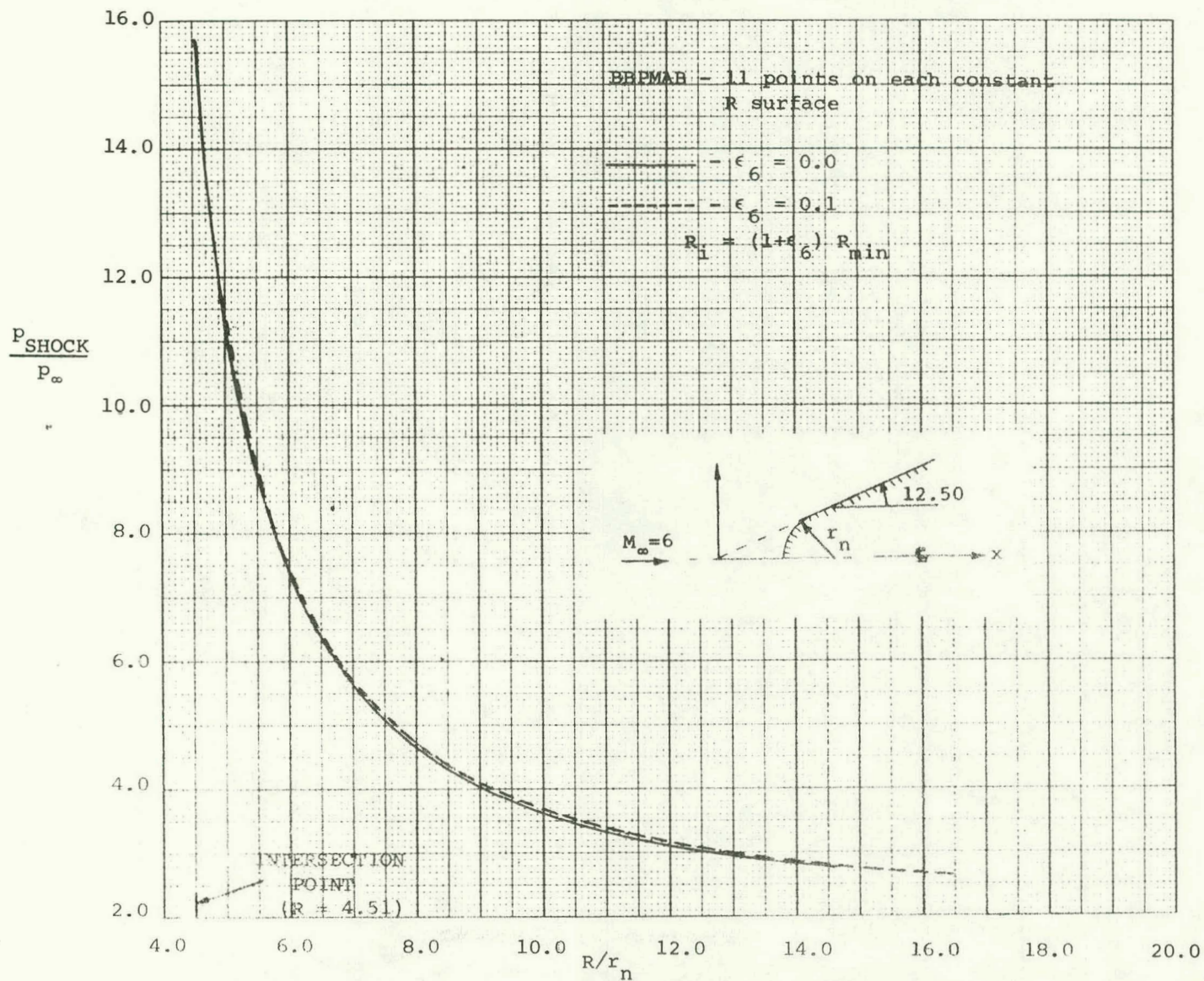
FIGURE 15: EFFECT OF ϵ_6 ON PRESSURE BEHIND SHOCK - SPHERICALLY TIPPED $12\frac{1}{2}$ DEGREE HALF-ANGLE CONE - ZERO INCIDENCE
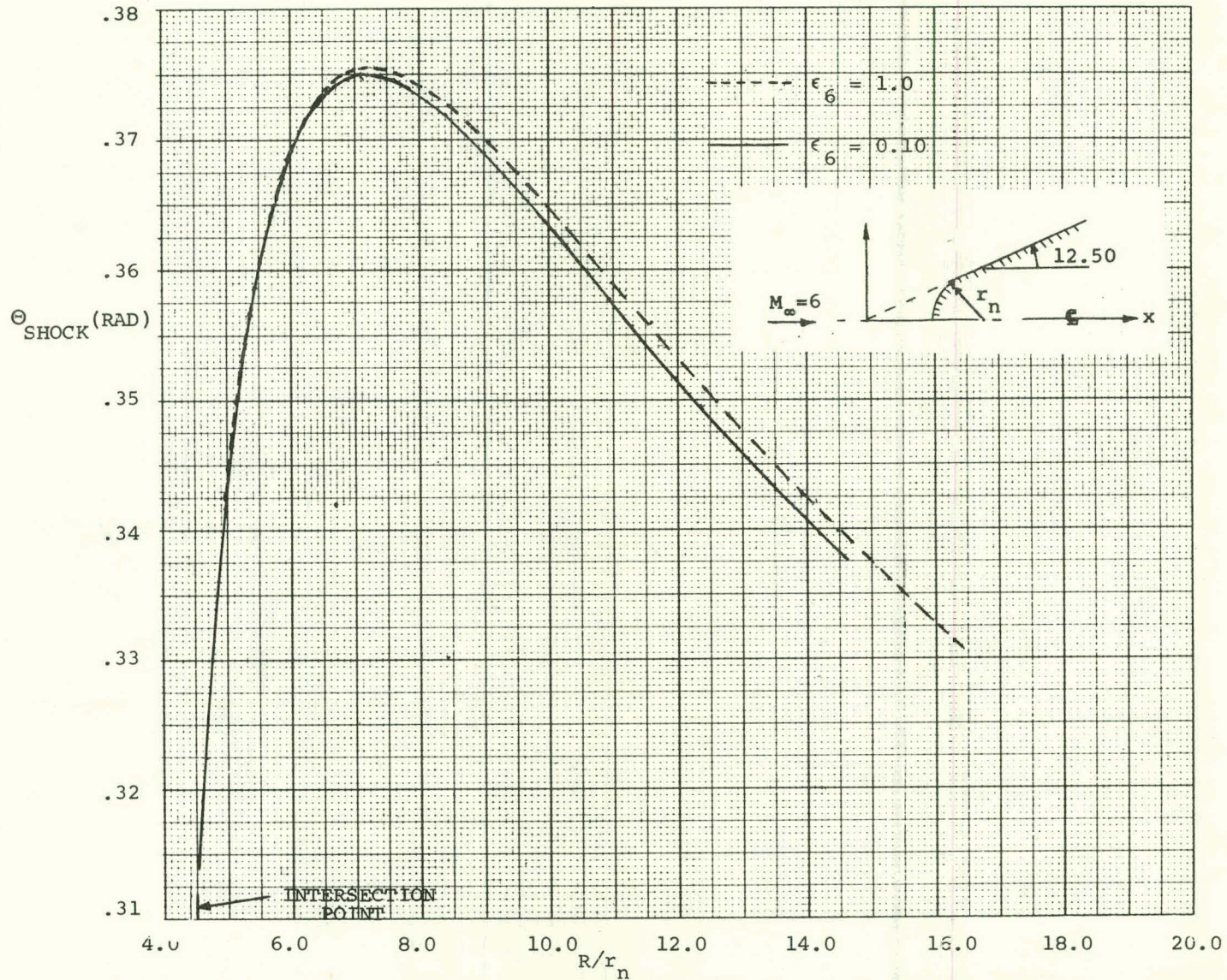
FIGURE 16: EFFECT OF ϵ_6 ON SHOCK POSITION - SPHERICALLY TIPPED $12\frac{1}{2}$ DEGREE HALF-ANGLE CONE - ZERO INCIDENCE
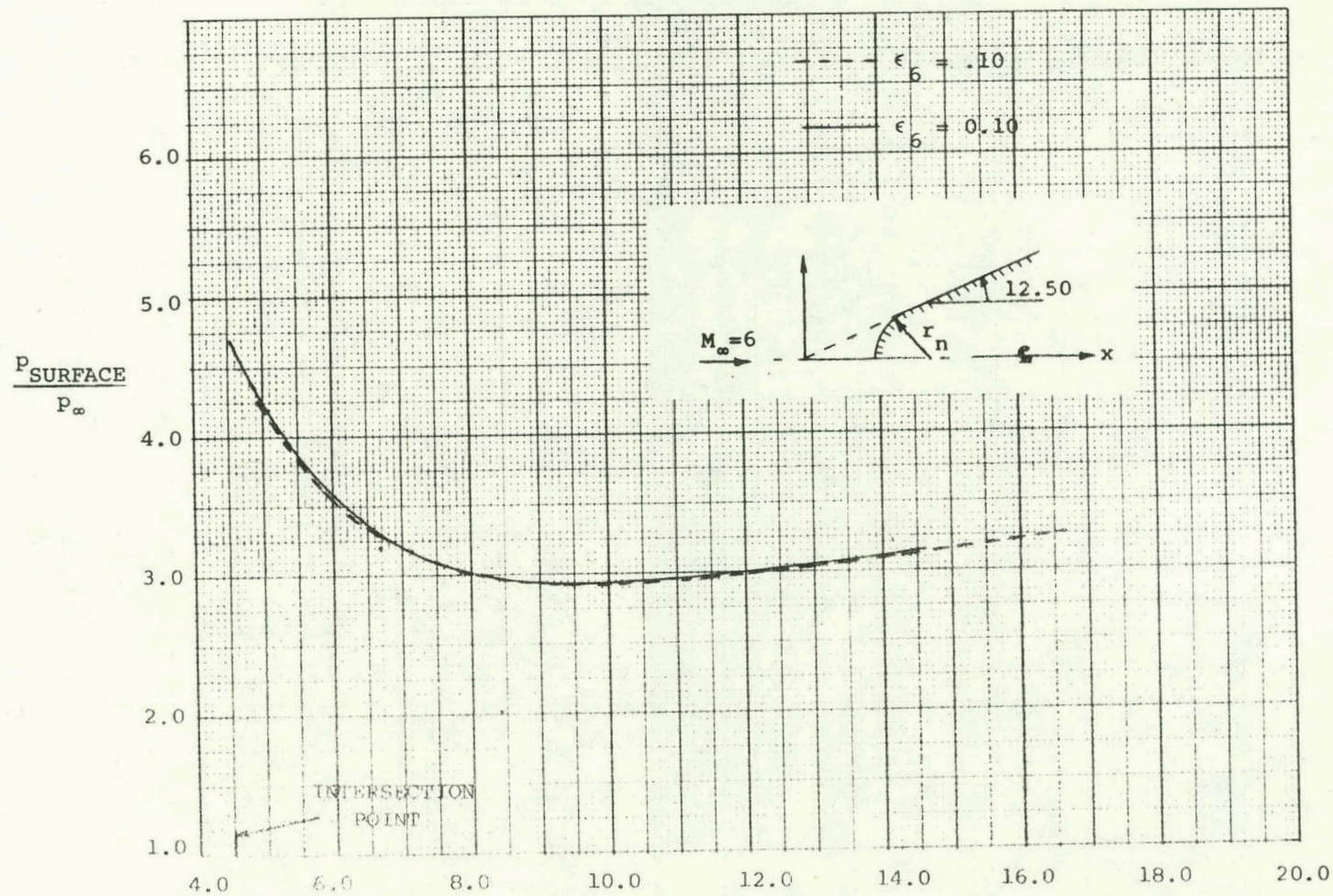
FIGURE 17: EFFECT OF ϵ_6 ON SURFACE PRESSURE – SPHERICALLY TIPPED $12\frac{1}{2}$ DEGREE HALF-ANGLE CONE – ZERO INCIDENCE
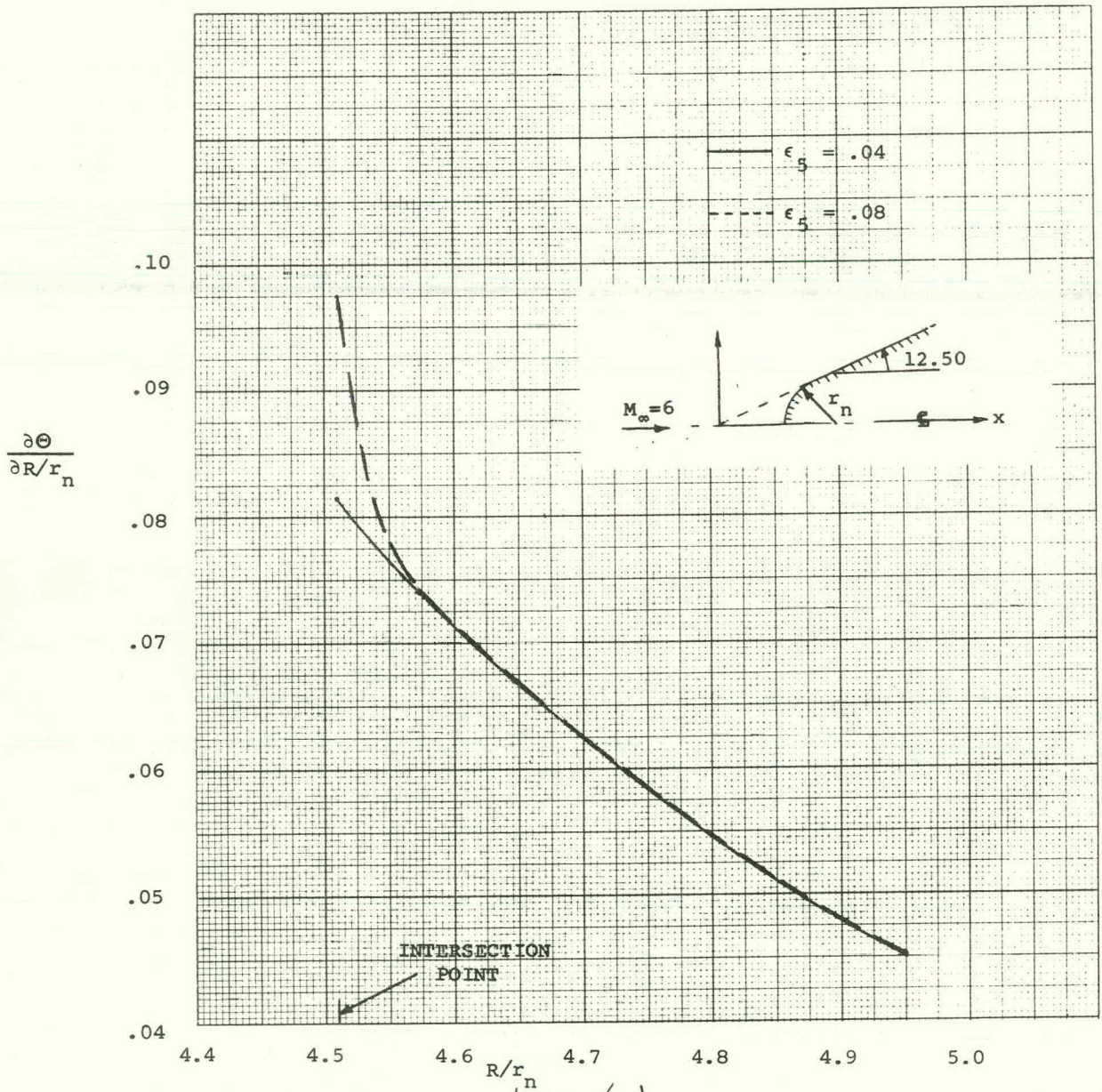
FIGURE 18: DEPENDENCE OF $\left(\partial\Theta/\partial R \Big/ r_n\right)_{SHOCK}$ ON ITS INITIAL VALUE-
SPHERICALLY TIPPED $12\frac{1}{2}$ DEGREE HALF-ANGLE CONE-
ZERO INCIDENCE
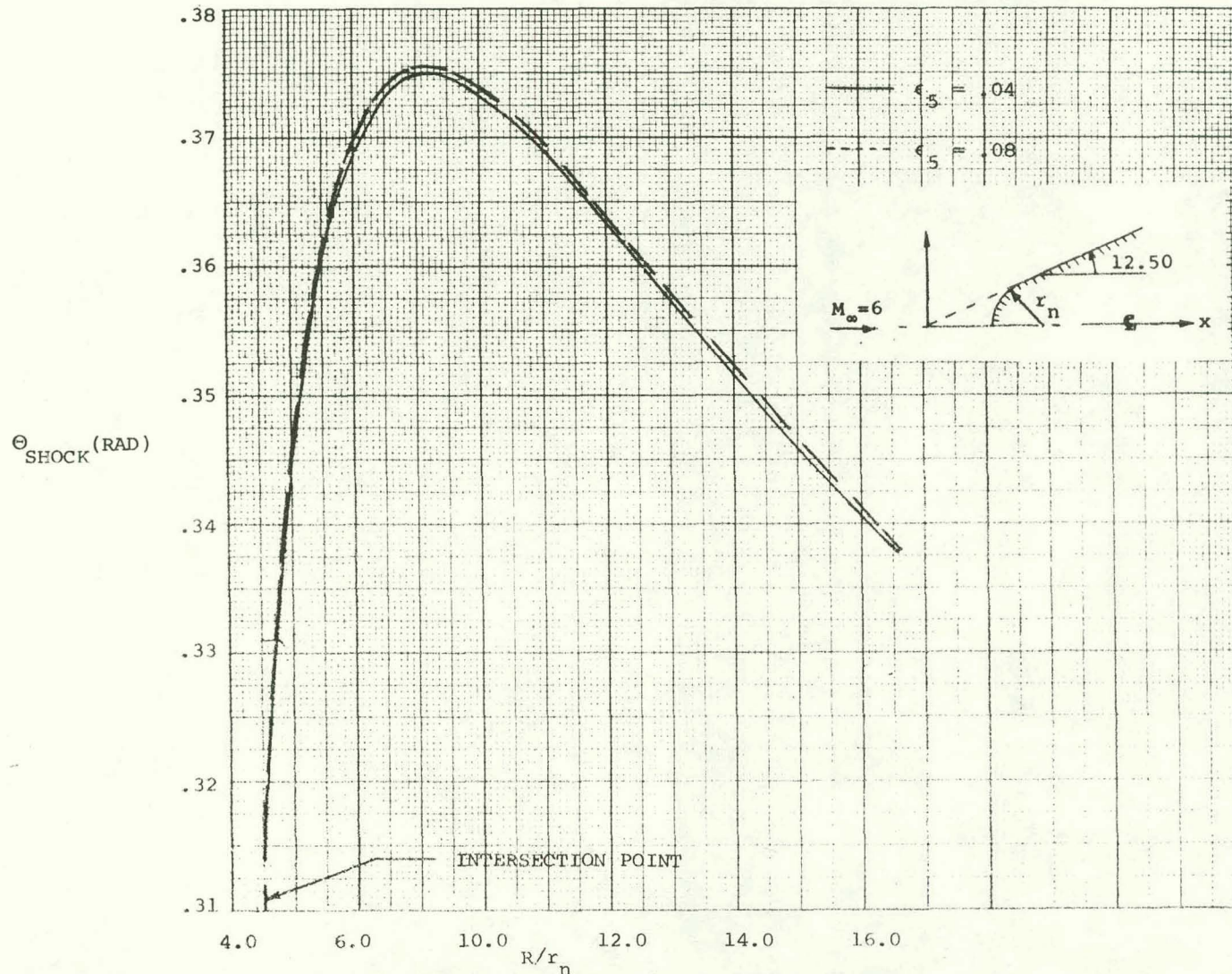
FIGURE 19: DEPENDENCE OF SHOCK ANGLE ON INITIAL VALUE OF $\partial\Theta_{SHOCK}/\partial R$ - SPHERICALLY TIPPED $12\frac{1}{2}$ DEGREE HALF-ANGLE CONE - ZERO INCIDENCE

DISTRIBUTION: (continued)
Cathryn C. Lyon
Head Librarian
U.S. Naval Weapons Laboratory (MAL)
Dahlgren, Virginia 22448

Jet Propulsion Laboratory
4800 Oak Grove Drive
Pasadena, California 91103
    Attn: Dr. Zenon Popinski

Aero-Physics Department
Raytheon Corporation
Bedford, Massachusetts 01730
    Attn: Fred Petri

Dr. Gino Moretti (5)
Polytechnic Institute of Brooklyn
Graduate Center - Route 110
Farmingdale, New York 11735

Ames Research Center
Moffett Field, California 94035
    Attn: John V. Rakich

Aero-Engineering Department
Wichita State University
Wichita, Kansas 67200
    Attn: Dr. Glen Zumwalt

Mike Abbett (5)
General Applied Science Laboratories, Inc.
Merrick and Stewart Avenues
Westbury, Long Island, New York 11590

Department of the Air Force
Air Force Aero Propulsion Laboratory (AFSC)
Wright-Patterson Air Force Base
Ohio 45433
    Attn: APO-4/STINFO Office

Physics International Company
2700 Merced Street
San Leandro, California 94577
    Attn: Helen Smith, Librarian

Knud Kindler
DVL-Institut fur Angewandte Gasdynamik
505 Purz-Wahn
Linder Hohe, Germany

Technion
Israel Institute of Technology
Central Library
Technion City—Haifa, Israel
    Attn: Mrs. A. Zadoks, Order Librarian

Dr. Samuel J. Cowan
Boeing Space Division
Box 3868
Seattle, Washington, 98124

Standard Aero-Thermodynamics
    Distribution (196)

J. A. Hornbeck, 1
D. B. Shuster, 1200
O. M. Stuetzer, 1220
L. D. Smith, 2300
R. S. Claasen, 2600
G. W. Rodgers, 2620
C. D. Ouverson, 2624
C. S. Williams, 2625
A. Narath, 5100
L. C. Hebel, 5200
C. R. Mehl, 5230
F. W. Neilson, 5240
E. H. Beckner, 5242
J. R. Banister, 5270
L. D. Smith, 5500
G. W. Anderson, 8330
G. A. Fowler, 9000
J. H. Scott, 9200
A. Y. Pope, 9300
R. C. Maydew, 9320
W. H. Curry, 9322
D. F. McVey, 9328
K. J. Touryan, 9340
J. K. Cole, 9341
    Attn: A. J. Russo
R. R. Eaton, 9341 (5)
W. F. Carstens, 3410
    Attn: W. J. Wagoner, 3413
    For: USAEC/TI (3)
        M. S. Goldstein (1)
B. R. Allen, 3421
B. F. Hefley, 8232
C. H. Sproul, 3428-2 (10)